Summer Internship 2013

Clean Technologies Research

PREC

PUERTO RICO ENERGY CENTER

PROGRAMA MASSIE
CHAIR OF EXCELLENCE
DE-NA0000672

August 19, 2013

August 19, 2013

SUMMER INTERNSHIP

Clean Technologies Research

2013

Editors

Suheilie Rodríguez González

Sandra R Pedraza Torres

Miguel Cotto Morales

Armando Soto

PREC

August 19, 2013

SUMMER INTERNSHIP

Clean Technologies Research

2013

Preface

The success of the 4th Summer Research Internship on clean technologies is ascribed to the efforts of Puerto Rico Energy Center (PREC) and Universidad del Turabo with the sponsorship of the Samuel P. Massie Chair Program of Excellence of the Department of Energy (DoE). During eigth weeks, thirteen students and eight mentors (professors, graduate students and industry representatives) participated conducting research on new technologies and solutions for solving the energy concerns that we face daily.

These proceedings include among others current issues of interest in areas such as biofuels, processes optimization, hydrogen production, nanotechnology . Seventeen proposals were reviewed by a multidisciplinary panel composed by professors and researchers of Universidad Interamericana, University of Puerto Rico and Universidad del Turabo. Sixty puertorican students applied pursuing a local internship experience.

We are grateful to the PREC team, to the Innovation and Commercialization Office and to the staff of Universidad del Turabo Vicechancellor Office for their contribution to accomplish successfully this experience.

Dr. Roberto Lorán
Principal Investigator
Samuel P. Massie Chair
Program of Excellence– DoE

Dr. Amaury Malavé
Executive Director
PREC

PREC

August 19, 2013

SUMMER INTERNSHIP

Clean Technologies Research

2013

CONTENTS

PREC

Biodiesel Production Utilizing Ultrasonic Processing

Bryan Santana Rivera
Universidad del Turabo, Gurabo, Puerto Rico, bsantana13@email.suagm.edu

Ian Gutierrez Molina
Puerto Rico Energy Center, Gurabo, Puerto Rico, igutierrez7@suagm.edu

Amaury Malavé
Puerto Rico Energy Center, Gurabo, Puerto Rico, ajmalave@suagm.edu

ABSTRACT

In this research, Biodiesel was produced utilizing ultrasonic processing on the transesterification reaction. Different types of vegetable oil (Canola & Corn) and pellet-type base catalyzers were utilized (KOH and NaOH) along with 99.8% methanol, to create potassium or sodium methoxide. The Ultrasonic processing set at full cycle & amplitude of 14.4 kHz were applied to the selected vegetable oil heated to 60°C and the methoxide of choice. The ultrasonic processing time varied between the biodiesel blends. The glycerin byproduct of the transesterification reaction was separated from the methyl esters (biodiesel) using gravitation and a separation funnel. Quality tests like the water & methanol tests were performed on the biodiesel blends to ensure completion of the transesterification reaction. Similarly, pH and viscosity tests were performed to ensure engine component longevity and proper compression-ignition engine operation. Additionally, the biodiesel blends were tested on a single cylinder compression-ignition test engine to determine the efficiency between the various blends.

Keywords: Ultrasonic, Transesterification, Vegetable Oil, Methoxide

1. INTRODUCTION

In recent years, an increase in the production of biodiesel has been developed. Biodiesel is an alternative to the increasing cost of petroleum and its derivatives, being a renewable, non-toxic, completely biodegradable fuel. Biodiesel emits significantly less amounts of hydrocarbons, carbon monoxide and particulate matter compared to petroleum diesel fuel, resulting in cleaner tailpipe emissions. Biodiesel contains 3.2 times the energy it takes to produce it. **[**1] Biodiesel is produced with vegetable oil, a base catalyzer (KOH, NaOH) & alcohol (methanol or ethanol). A transesterification reaction occurs between the vegetable oil and the methoxide, (potassium or sodium), producing a methyl ester (biodiesel) and glycerin. The average completion time of the standard transesterification reaction is from 45 minutes to 2 hours, depending on factors like reaction temperature & the amount of catalyzer utilized. Utilizing an ultrasonic processor causes the formation & collapse of fluid bubbles, called cavitation. The formation & collapse of these bubbles releases energy, resulting in reduced transesterification reaction time and increased mass transfer rate. [2] In this research, the adequate preparation procedures for biodiesel utilizing an ultrasonic processor were studied, along with a comparison of emissions between different biodiesel blends, utilizing a single cylinder test engine.

1.2 EXPERIMENTAL PROCEDURE

In this research, two types of vegetable oil were utilized, Corn & Canola Oil. Each oil sample was heated to 60°C before mixing with the methoxide of choice (sodium or potassium). The methoxide was prepared by mixing 99.8% pure methanol and the selected pellet-type base catalyzers (NaOH & KOH), until the catalyzer was fully dissolved in the methanol. A Hielscher UP400S ultrasonic processor was utilized to mix the selected vegetable oil with the

methoxide of choice. The ultrasonic processor was set at 60% (14.4kHz) amplitude & full cycle on all tests. However, the ultrasonic processing times vary between the blends.

After the ultrasonic processing and transesterification reaction are completed, the biodiesel is placed in a separation funnel and left for 10 hours to insure complete separation from the glycerin, which is separated from the biodiesel by gravitation.

Biodiesel is subjected to two quality tests: the water and methanol tests, which test for the completion of the transesterification reaction during the ultrasonic processing. The water test is realized using a 1:1 biodiesel/water ratio, mixing them for 10-20 seconds until a homogeneous mixture is achieved; the water should separate at the bottom completely from the biodiesel in 0.5 hours or less, indicating a complete reaction. The Methanol test is realized using a 5:45 biodiesel/methanol ratio, mixing both components and letting it settle for 10 minutes. Any unprocessed oil will settle at the bottom of the container indicating an incomplete reaction, otherwise, the reaction is complete. To ensure the longevity of some engine components, the biodiesel should possess as much of a neutral pH level as possible. To obtain adequate pH values, the biodiesel is washed continuously with warm water until the pH is at the desired level, with an amount of warm water that represents 1/3 of the total biodiesel volume. Viscosity tests at 40° C were performed on the biodiesel utilizing an Ostwald viscometer, ensuring the biodiesel complies with the ASTM D-445 test for adequate viscosity levels (1.9cSt - 6.0cSt) for operation in a compression-ignition engine.

2. RESULTS AND DISCUSSIONS

Twelve biodiesel blends were produced, with different oils, amounts of catalyzer and methanol. Two blends were selected as potential quality fuels, although the Mark 3 of needed to be reprocessed. The reprocessing consisted of a 30% increase in catalyzer & methanol amount, including an additional 20 minutes of ultrasonic processing. After reprocessing, the methanol and water quality tests [3] were re-performed netting successful results, indicating a complete transesterification reaction.

During the production of the methoxide, it was noticed that the sodium hydroxide (NaOH) took an increased amount of time to dissolve in the methanol when compared with the potassium hydroxide. Therefore, it's advised to use potassium hydroxide for quicker methoxide processing.

Table 1: Produced Biodiesel blends Specifications

Blend	Methanol (mL)	Catalyzer (g)/Type	Oil (mL)/Type	Processing Time (Total)
Mark 3.1	130	1.30 (NaOH)	500 (Canola)	30 min
Mark 11	130	5.8 (KOH)	500 (Corn)	20 min

Table 2: Produced Biodiesel blends Viscosity and pH readings

Blend	Viscosity (cSt)	PH Readings
Mark 3.1	5.068	6.92
Mark 11	5.054	6.68

All of the blends showed results for viscosity and pH in the correct range for proper operation in a compression-ignition engine. After the quality tests were completed, the biodiesel blends were tested on a Gunt Hamburg CT-110 single cylinder compression-ignition test stand engine. The purpose of the test was to obtain live data from the produced biodiesel blends and compare it against the commercially available diesel fuels at the pump. All Tests

were performed at 6.5 N/m of torque and 2998 Rev/min. various parameters were logged while testing the blends on the test engine; the most utilized in this research is the efficiency of the engine. The commercially available diesel fuels were tested, calculating the average efficiency of the blends and identifying the less avg. efficient diesel, which was the local Total diesel as seen on table 3 and illustrated on Figure #1.

Table 3: Commercially available Diesel fuel Efficiencies (%)

Time (min)	Puma Diesel fuel Efficiency (%)	Total Diesel fuel Efficiency (%)
1	25.544	22.9148
2	25.6776	38.8411
3	19.8194	15.5749
4	23.6495	20.1231
5	35.3458	14.1742
6	23.727	23.5781
Average Efficiency	25.65%	22.53%

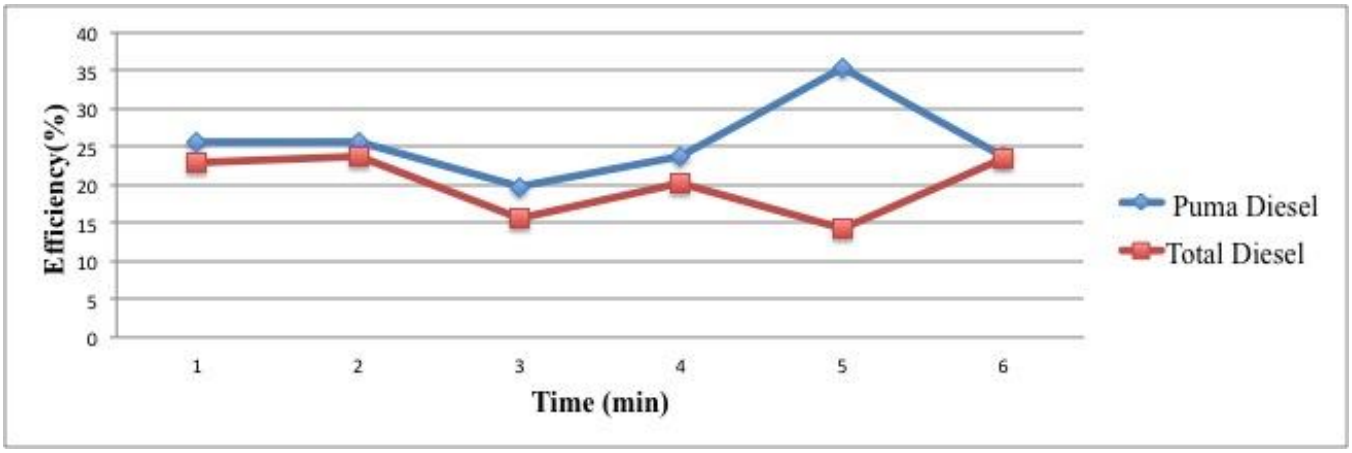

Figure 1: Commercially Available Diesel Fuels Efficiency (%) vs. Time (min)

Since the authors were still testing the appropriate method for producing biodiesel, the multiple blends were produced in scaled amounts in order to save materials. Therefore, a low amount (mL) of each blend of biodiesel was produced. To provide a broader range of real-world testing, each blend was tested using a B20 blend, in which 20% of the total volume represents the selected biodiesel blend, while the other 80% would be composed by the Total diesel, being the less average efficient commercially available diesel fuel as shown on Figure 1. Results showed that the B20 Mark 3.1 blend had the highest average efficiency between the B20 blends tested as shown on Table 4 and Figure 2. Also, the B20 Mark 3.1 biodiesel blend had a 1.92% increase in efficiency and the B20 Mark 11 also had a 1.25% increase when compared to the efficiency of the Total diesel fuel. B20 blends are sold at the pump on the U.S. and are commonly used by the owners of diesel engine powered vehicles, reporting no loss in fuel economy, while having a 21.1% reduction in hydrocarbons, 11.0% reduction in carbon monoxide and a 10.1% reduction in particulate matter when compared to standard diesel fuel, according to EPA. [4]. The Mark 3.1 and 11 Blends were tested using a B100 blend, in which the biodiesel covers 100% of the total volume of the fuel. Results clearly showed that the B100 Biodiesel Mark 3.1 was the most efficient throughout the test, as seen on Figure 3. An

increase of 5.6% in efficiency levels on the B100 Mark 3.1 was noticed when compared to the efficiency levels of the Total diesel fuel.

Table 4: B20 Biodiesel blends Efficiencies (%)

Time (min)	B20 Mark 3.1 Biodiesel blend efficiency (%)	B20 Mark 11 Biodiesel blend efficiency (%)
1	21.7708	22.9027
2	30.5539	22.8151
3	20.8009	22.4034
4	26.2199	23.4035
5	18.1864	26.3705
6	25.20	28.8052
Average Efficiency	24.45 %	23.78%

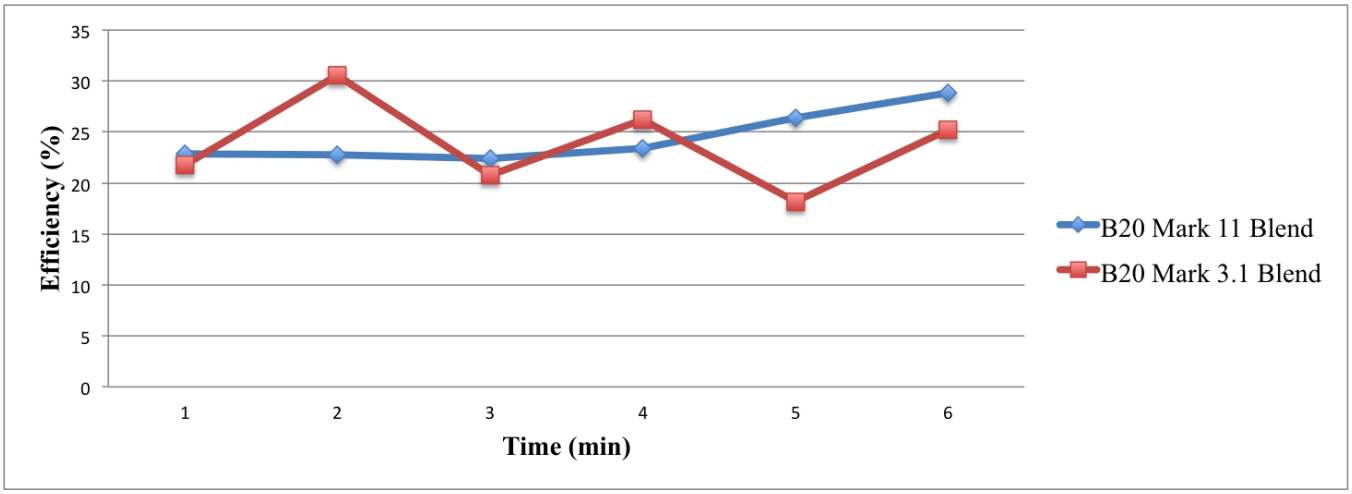

Figure 2: Efficiency of B20 Biodiesel Blends vs. Time (min)

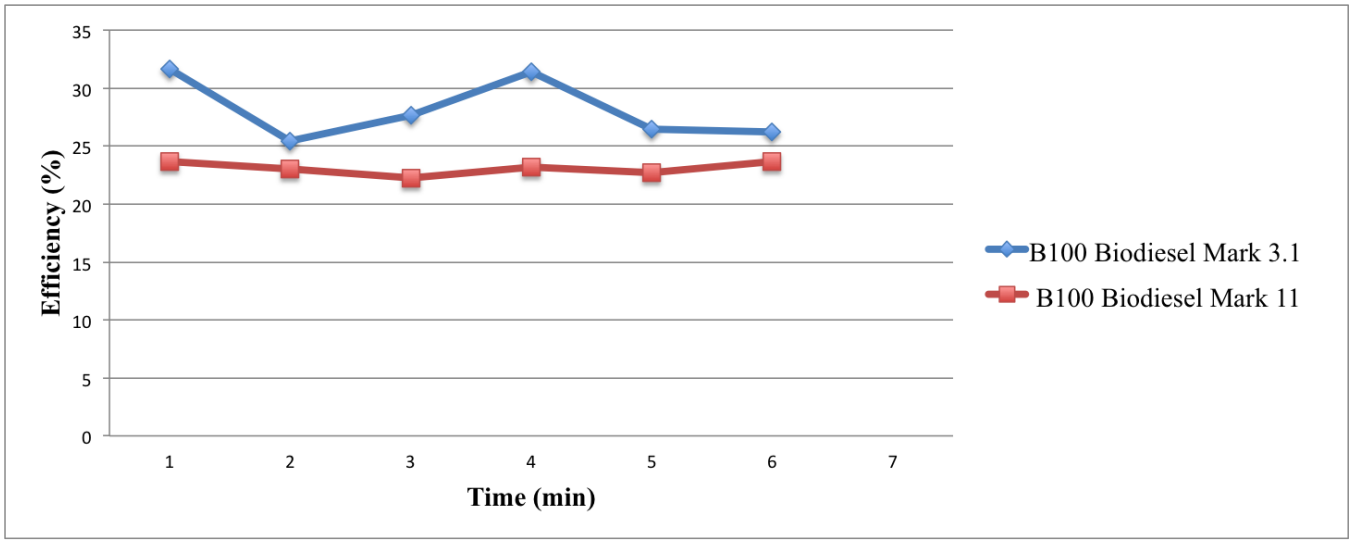

Figure 3: B100 Biodiesel Blends Efficiency (%) vs. Time (min)

An Infralyt CL exhaust gas analyzer was utilized to record exhaust emission data during the operation of the Gunt Hamburg CT-110 single cylinder compression-ignition test engine with the various diesel blends. The Carbon Monoxide (CO) and Hydrocarbon (HC) content data obtained from the analyzer were analyzed for comparison between the Total diesel fuel & B20/B100 biodiesel blends produced. For Hydrocarbon (HC) Content, the B20 blends had an average reduction of 18.48% (B20 Mark 3.1) and 20.09% (B20 Mark 11). Additionally, the B100 blends had an average reduction of 57.07% (B100 Mark 11) and 54.89% (B100 Mark 3.1) when compared with the hydrocarbon (HC) levels emitted by the Total diesel fuel, as shown on Figure 4. During the testing a reduction in tailpipe combustion smell, was noticed with the B20 blends but the highest reduction was noticed with the B100 blends, in comparison with standard diesel fuel. For Carbon Monoxide (CO) content, the B20 had an average reduction of 13.99% (B20 Mark 3.1) and an average increase of 1.18% (B20 Mark 11). Additionally, the B100 blends had an average reduction of 92.69% (B100 Mark 3.1) and 44.35% (B100 Mark 11) when compared to Carbon Monoxide (CO) contents emitted by the Total diesel fuel, shown on Figure 5.

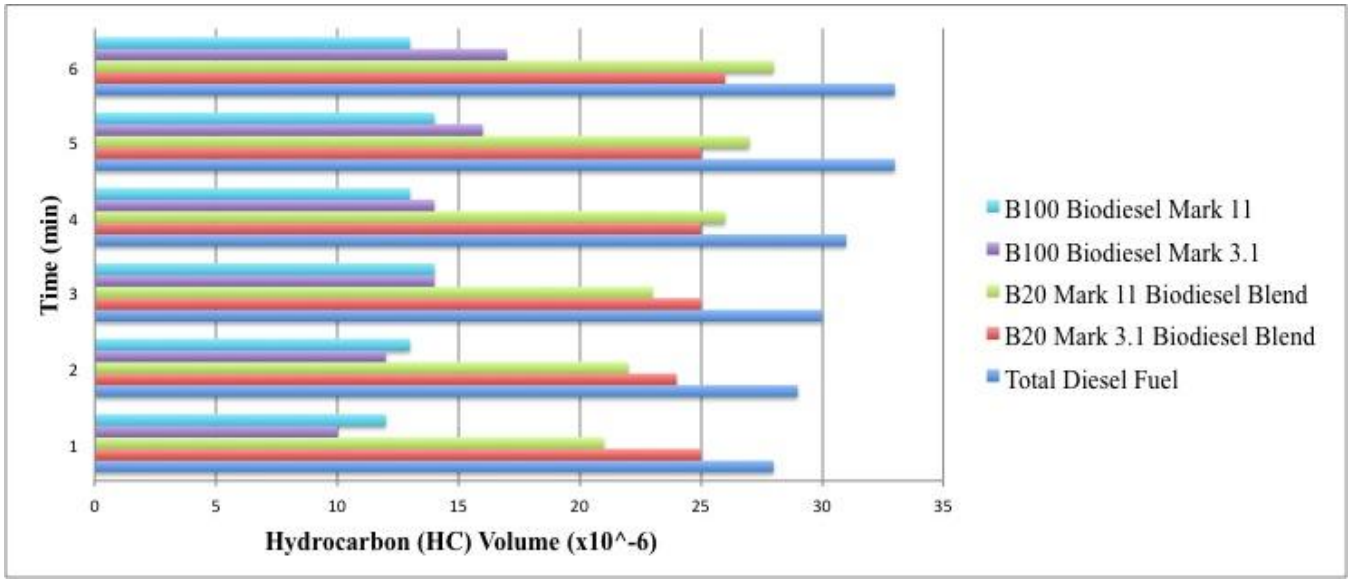

Figure 4: Hydrocarbon Volume Emissions for Diesel, B20 & B100 Biodiesel Blends vs. Time (min)

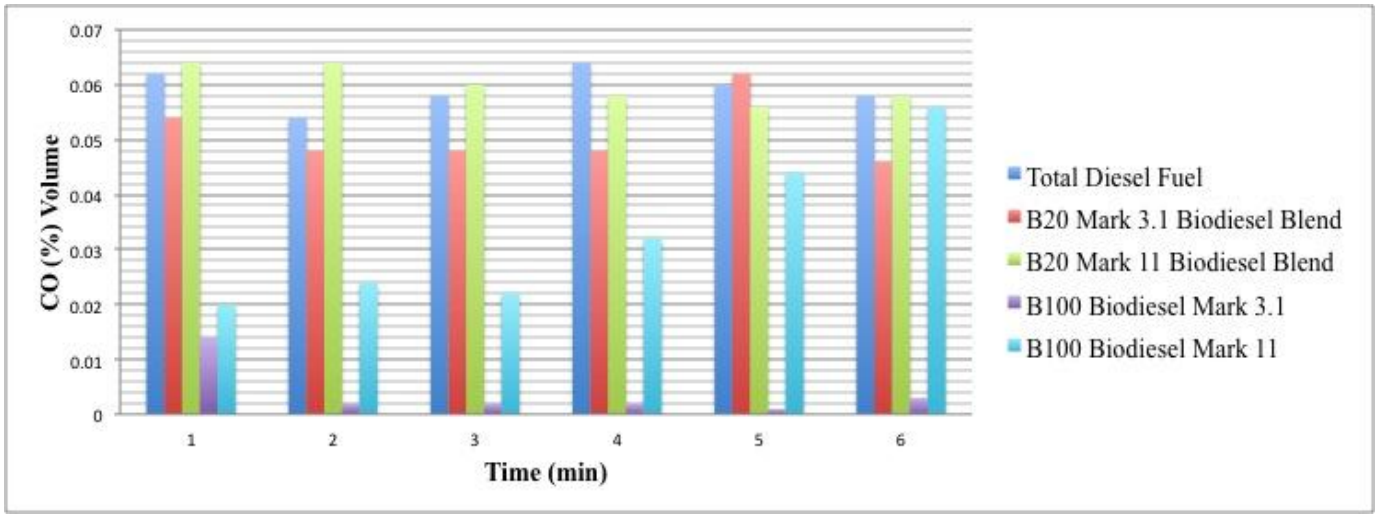

Figure 5: Carbon Monoxide (CO) Emission Levels of B20 and B100 Biodiesel Blends vs. Time (min)

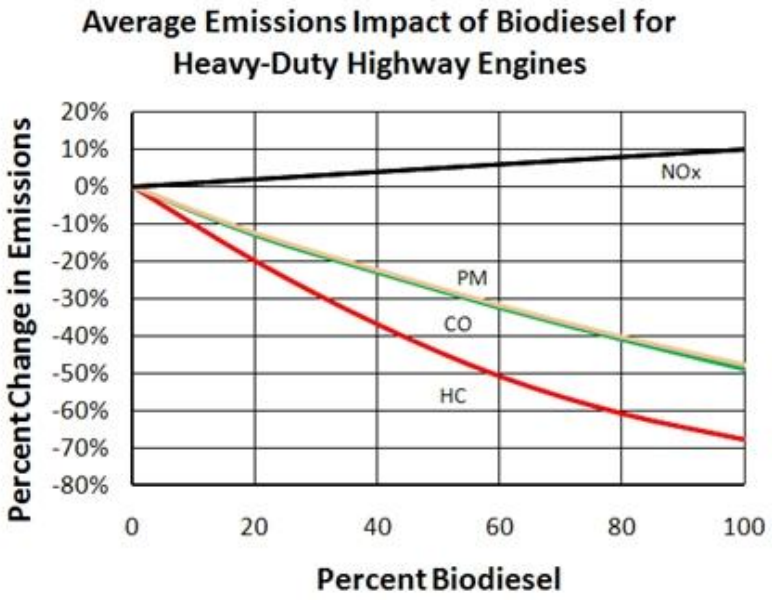

Figure 6: Reduction Percentage (%) of Emission Levels vs. Biodiesel Percentage (%) of Total Volume [4]

3. CONCLUSIONS

Biodiesel can be produced successfully using an ultrasonic processor, reducing the completion time of the transesterification reaction by 85%, compared to the standard procedures for the transesterification reaction. The use of the Potassium Hydroxide base-catalyzer reduces methoxide-processing time requiring 75% less time to dissolve on methanol, when compared to the sodium hydroxide base catalyzer. Ultrasonic processing was applied to the heated oil and methoxide of choice at full cycle and 14.4 kHz of amplitude, with varied processing times. Quality, pH and Viscosity tests were performed to ensure adequate operation on a compression-ignition engine. The Biodiesel blends were mixed on a B20 Biodiesel ratio and B100 Biodiesel. Increased efficiency numbers, ranging from (1.5% to 5.4%) were found on all the biodiesel blends (B20 & B100) when compared to standard diesel fuel. An Infralyt Cl exhaust gas analyzer was utilized to compare the Hydrocarbon (HC) and Carbon Monoxide (CO) levels of the standard diesel fuels and the produced biodiesel and blends. An average reduction in Hydrocarbon (HC) levels ranging from (18%-20%) for B20 Biodiesel blends and (54%-57%) for B100 Biodiesel. Accordingly, reduction for Carbon Monoxide B20 blends had an average reduction of 13.99%, while B100 had reduction ranging from 44.35%-92.69%. During the emission testing, it was noticed that as the volume of biodiesel in substance increases the emission smell is reduced considerably due to reduced emissions as seen on Figure 6, especially on the B100 Blends. Future plans include but are not limited to: a further investigation on cavitation, to see how this process affects the transesterification reaction. Also, studies on how to make biodiesel more emissions free and efficient, to improve its energy content.

REFERENCES

[1] United States DOE: Alternative Fuels Data Center (2013) Biodiesel Benefits and Considerations, http://www.afdc.energy.gov/fuels/biodiesel_benefits.html 06/13/13 Accessed

[2] Larpkiattaworn, S., Jeerapan, C., Tongpan, R. and Tongon, S. (2010) "Ultrasonic on transesterification reaction for Biodiesel production", Research, Thailand Institute of Scientific and Technologic Research, Pathum Thani, Thailand.

[3] Addison, K. (2001). Biodiesel Quality Tests, http://journeytoforever.org/biodiesel_vehicle.html#washtst, 06/04/13 Accessed.

[4] United States Environmental Protection Agency. (2002). A Comprehensive Analysis of Biodiesel Impacts on Exhaust Emissions.

[5] Knothe, G., Van Gerpen, J. and Krahl, J. (2005). *The Biodiesel Handbook*, 1st Edition, AOCS Press, Illinois, U.S.A.

Authorization and Disclaimer

Authors authorize PREC to publish the paper in the internship proceedings. Neither PREC nor the editors are responsible either for the content or for the implications of what is expressed in the paper.

Gas Turbine Health Monitoring: Part 1, Turbojet Engine Construction

Gelson Díaz
Universidad del Turabo, Gurabo, PR, USA, g_diaz_12@hotmail.com

Sigfredo Nieves
Universidad del Turabo, Gurabo, PR, USA, sigrx73@hotmail.com

Miguel Delgado

Universidad del Turabo, Gurabo, PR, USA, m_delgado_01@hotmail.com

Edwar Romero
Universidad del Turabo, Gurabo, PR, USA, eromero@suagm.edu

ABSTRACT

The goal of this project is to build a turbojet engine for experimentation. Commercial turbojet engines are cost prohibitive while educational versions still cost over tens of thousands of dollars. A less expensive solution is to build one using an automotive turbocharger as the core component. The turbocharger is a practical choice since it already has a compressor and turbine, requiring only the construction of the combustor and related accessories for operation.

Keywords: Turbojet engine, turbocharger, gas turbine

1. INTRODUCTION

A gas turbine, or combustion turbine, or turbojet is a type of internal combustion engine. This engine is composed of a compressor, a combustion chamber, and a turbine. The combustion chamber, or combustor, is located in-between the compresor and turbine sections. The operation of a gas turbine is similar to a steam power plant, being the only difference that it uses air instead of water vapor. When air flows through the compressor section, it increases the pressure. In the combustor, fuel is added to the air producing an air-gas mixture. The ignition of this mixture creates a high-temperature and high pressure flow. This gas flow enters the turbine, the expanding exhaust gases produces useful work output. The shaft work output can be used to drive an electric generator for power generation or to produce thrust for aircrafts.

The gas turbine process can be analyzed as a Brayton cycle. Gases circulating on an ideal gas turbine undergo three thermodynamic steps: an isentropic compression, an isobaric (or constant pressure) combustion and isentropic expansion (Cengen & Boles). Fig. 1 depicts a sketch of this process.

Gas turbines are known to present reliability problems due to shaft and blade misalignments that can lead to severe vibrations and costly rotor damage (Hall & Mba, 2003). Torsional vibrational monitoring has been identified as one technique capable of detecting changes in natural frequency for health monitoring (Maynard et al, 2001). Then, an energy harvesting system with torsional vibrating monitoring for turbine shaft placement is proposed. The Energy Harvesting Research Group (EHRG) at Universidad del Turabo is developing an energy harvester for this application and a monitoring device. Thus, a gas turbine is required for experimentation.

Since commercial gas turbine designs are typically used in large scale power plants and aircrafts, their cost is prohibitive. Educational gas turbine also cost tens of thousands of dollars. On the other hand, fabricating a gas turbine using an automotive turbocharger (compressor + turbine) is a less expensive option for this project. Thus, automotive components and mechanical design of gas turbines are required for the first part of the project. Most

of the information for custom-built gas turbine come from amateur or hobbyst designs. This project uses the Experimental Jet Turbine guidelines from RCDON for design purposes.

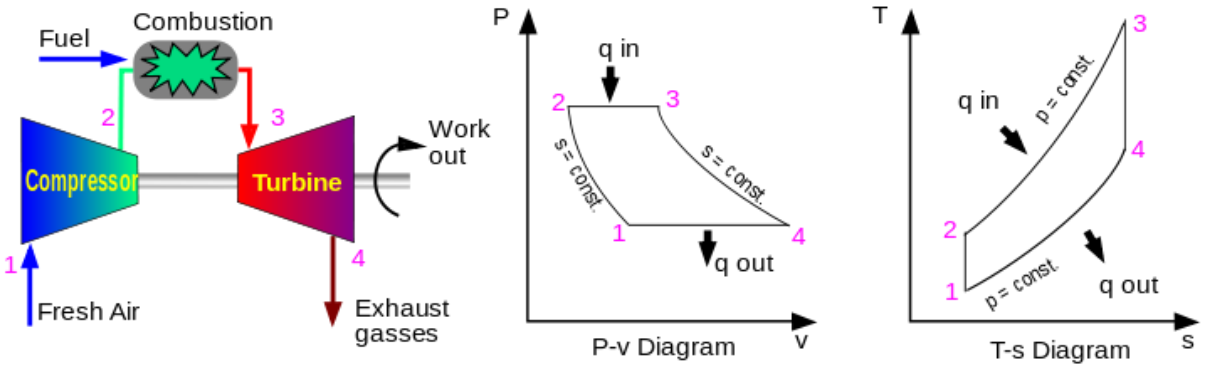

Figure 1: Theoretical Sketch and Graphs of a Gas Turbine

2. CONSTRUCTION

A turbocharger, automotive components, stock carbon steel pipes and plates, aluminum and brass rods were identified as the materials to be used.

2.1 TURBOCHARGER

The turbocharger is from a Dodge Diesel Ram truck. To be more specific, is the model "HX35W T3 Flange Dodge Ram 2500 / 3500 TURBO CHARGER". The main objective at the moment of choosing the turbocharger model, was its low cost in case of a turbo meltdown. Fig. 2 shows a picture of the turbocharger choosen, while Table 1 presents its specifications.

Figure 2: Turbocharger

Table 1: Turbocharger Specifications

Description	Compressor Section	Turbine Section	Application
4” Inner Diameter (I.D.)	8 Blades	3” DIA to Flange	Brand New
Wet Floating Bearings	2.05” I.D.	2.5” I.D. Exhaust	1994-2001 Dodge Ram 2500/3500
Oil Inlet M12x1.5	3.27” O.D.	2.76” I.D.	
T3 Flange, Compressor outlet to 2” I.D. and 3” Outer Flange		2.36” O.D.	

2.2 MATERIALS

Table 2 shows a list of the stock materials used in this project including description and costs. Table 3 lists the automotive components and accessories used along this project including the associated costs.

Table 2: Materials Specifications

Material	Description	Cost
Low-Carbon Steel	1" X 1" squared pipe	$106.60
	4" diameter pipe	$24.68
	3" diameter pipe	$20.87
	2" X 1/8" plate	
	4" X 1/4" plate	
Aluminum	3" diameter X 3" long rod	$15.00
Brass	1-1/4" diameter rod	

2.3 FRAME

The frame was built using 1” x 1” square-section of low-carbon steel tube. The frame was designed with dimensions of 18.5” H x 20”W x 36” L in order to hold all the components of the gas turbine. The size was chosen to allow ample free space for handling and for modifications. Figure 3 shows the construction process while Fig. 4 presents an schematic for the frame layout designed in SolidWorks.

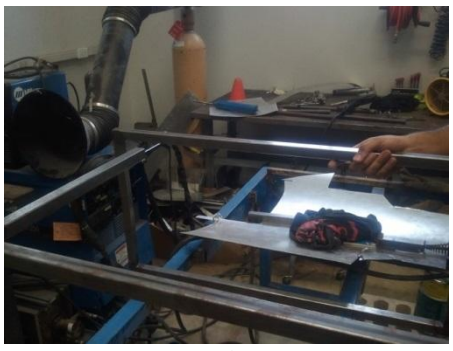

a)

b)

c)

Figure 3: Frame Construction Process. a) Side position of the frame for welding, b) Complete frame assembly, c) Measuring the frame

Table 3: Component Specifications

Equipment	Description	Qty.	Cost
Turbocharger	CUMMINS Dodge Diesel RAM 6BTAA 5.9L HX35W 3538881 Turbo Charger 6BT	1	$299.00 + $28.00 shipping
Turbo Flange "plate"	N/A	1	$20.00
Oil Cooler	Hayden Automotive cooling system	1	$100.96
Oil Catch Can	Oil catch tank/can with breather	1	$79.95
Spark Plug & Cable	Generic car part	1	$23.98
Ignition Coil	MSD Blaster 2 Ignition Coils 8202	1	$39.95
Condenser and bolt	N/A	1	$15.00
Fuel Pressure meter	After market gage car parts	1	$16.99
Oil Pressure meter	After market gage car parts	1	$24.99 + $10.00 shipping
Air Pressure meter	After market gage car parts	1	$57.99
Oil Pump	12V Electrical pump	1	
12V DC motor	RadioShack DC motor	1	$7.00
Oil Hose	Generic car part	1	
Fuel Hose	Generic car part		
Air Hose	Generic car part	1	$16.05
V-Clamp	V-band clamp kit 2.5" with 2pc steel	1	$28.00
T-bolt clamp	T-bolt clamp 3.00'	2	$10.00
Kill Switch	N/A	1	$4.98
Switches	RadioShack switches	4	
Solenoid	ACE CREW 12 VDC Solenoid	1	
Gas Cylinder	15 lbs. gas cylinder	1	
Paint	Enamel spray paint	3	
Battery	12V car battery "Econo Power"	1	$72.00
Oil Filter	Fram oil filter (generic car part)	1	$4.19
Battery Poles	Generic car part	2	
Electric Cables	Wire primary 16GA 28	1	$6.99
Gas Blower-Vac	RYOBI 2 cycle gas blower-vac		
Oil	10W40 "Proline" car oil	2	$8.38
Battery terminals	Terminal HD universal epoxy	1	$5.99

2.4 OIL SYSTEM

The use of an oil pump in line with an oil filter is required to lubricate the turbine while in operation to avoid the burning of the bearing systems. Fig. 4 shows the components positioning inside the frame. Figures 5 to 12 present the placement of the actual components.

2.5 BATTERY AND TURBINE POSITIONING

The battery is positioned to the back of the frame, closer to the powered components. The turbocharger is located to the front of the frame where the hot air can escape without obstructions and away of other temperature sensitive components. This will also add safety for operation of the turbine. Fig. 13 shows the turbocharger location while Fig. 14 indicates the battery placement. Figure 15 shows a picture of the battery support inside the frame.

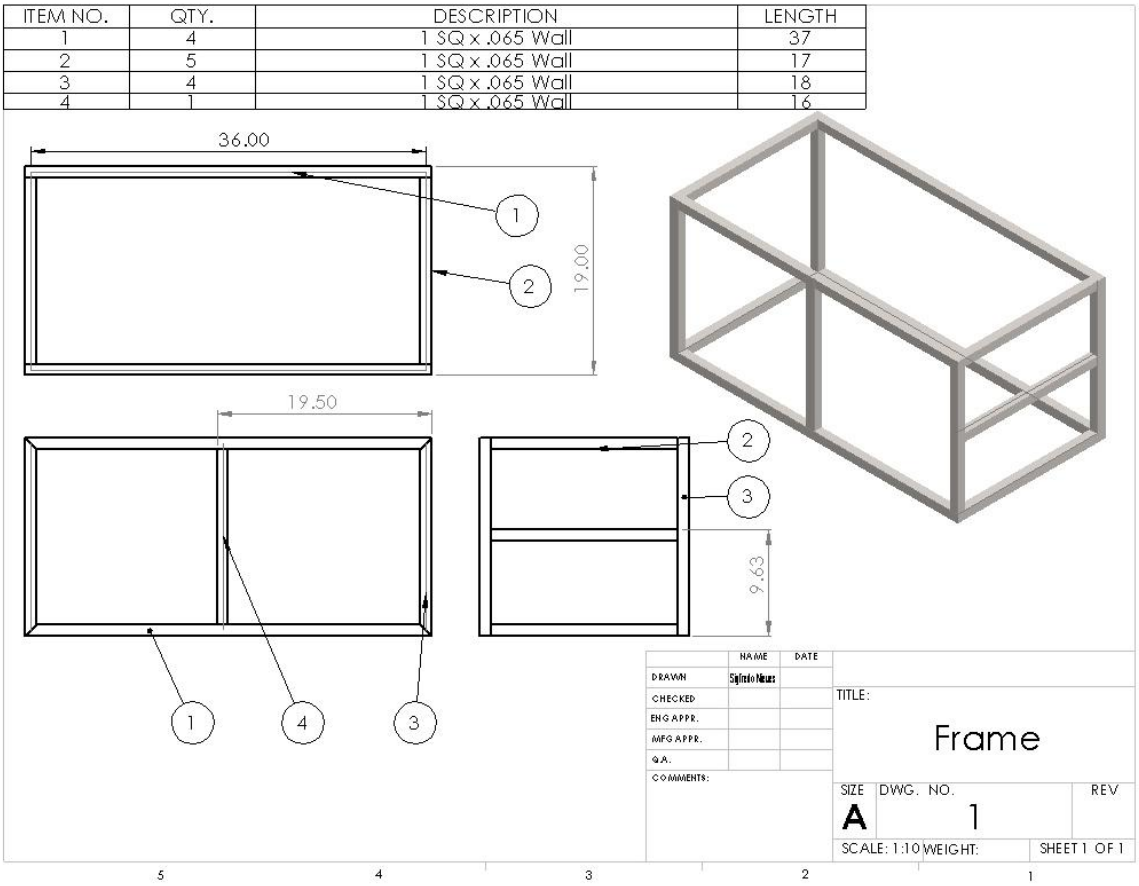

Figure 4: Frame cutting list (Inches). The frame has four different length of tube each one is numbered by his length.

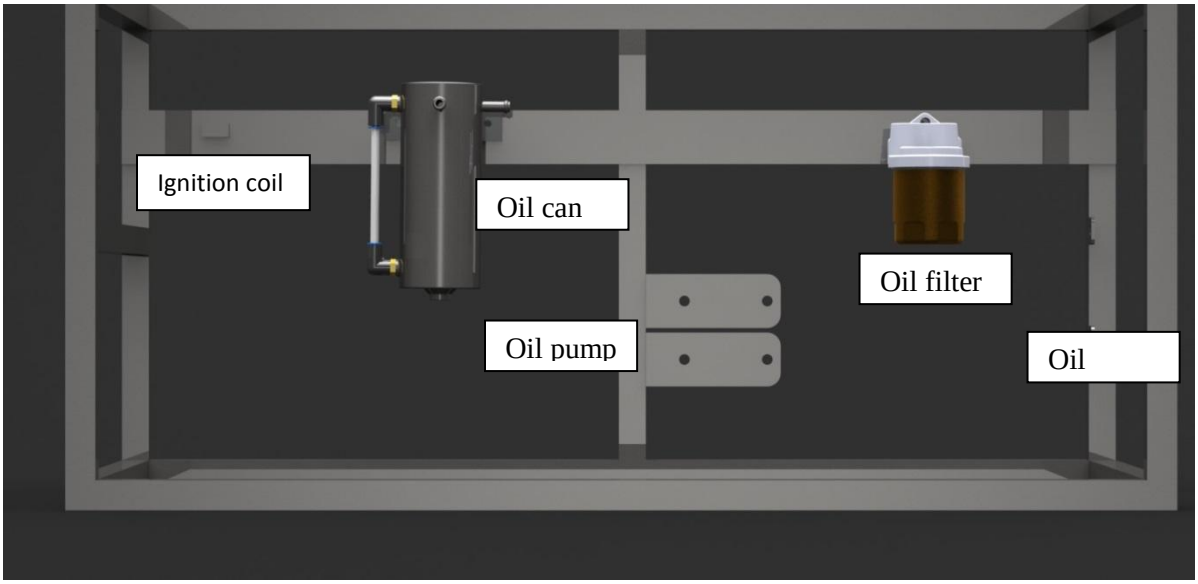

Figure 4: Oil system components positioning

Figure 5: Two plates of 2 ”L x 1” W x 1/8” thicknesses welded to the frame to mount the oil cooler.

Figure 6: A rectangular plate of 2”W x 1/8” thickness welded to mount the ignition coil, oil filter and the oil catch can.

Figure 7: View of the mounting plate welded to the frame.

Figure 8: Installation of a fence to one side of the frame to protect the oil cooler

Figure 9: View of the oil cooler mount.

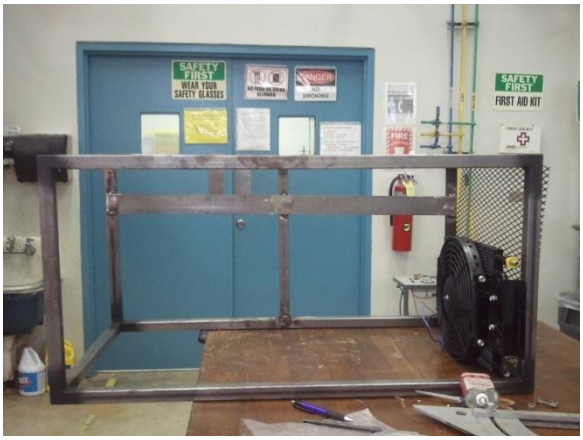

Figure 10: Front view of the frame.

Figure 11: Oil cooler placement.

Figure 12: Assembly of the oil cooler and safety screen.

Figure 13: Oil filter and oil catch can positioned with screw to the rectangular plate

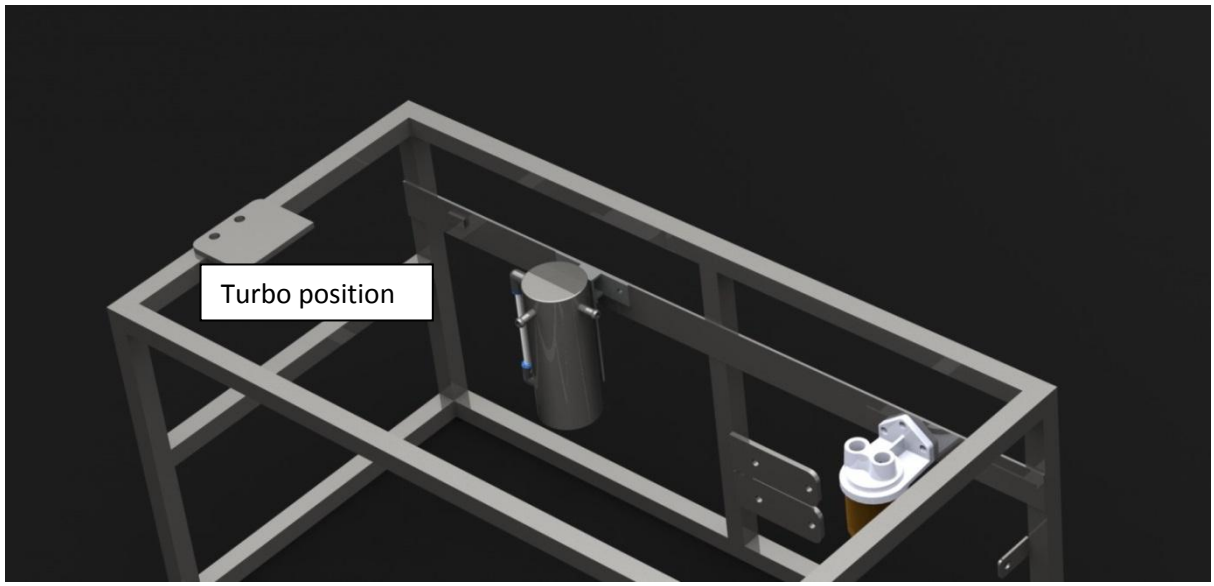

Figure 14: Turbocharger placement

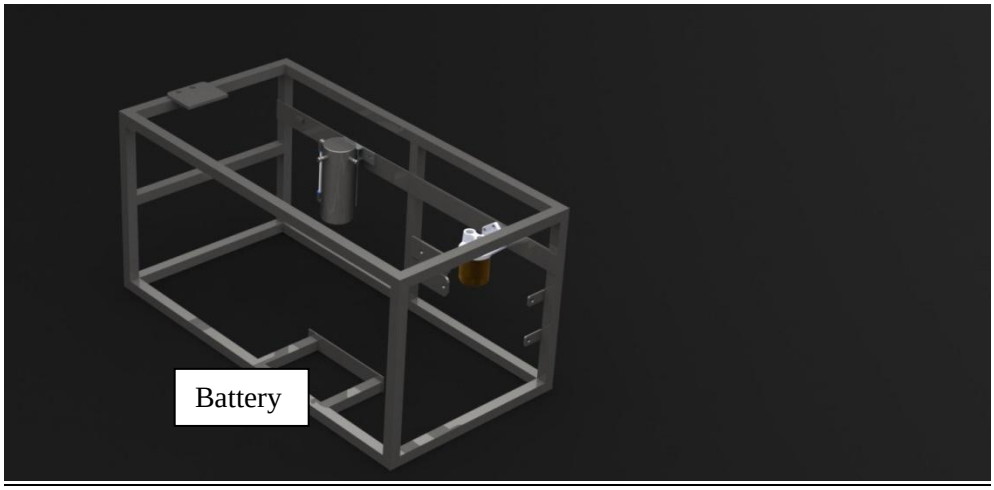

Figure 15: Battery placement

Figure 16: Battery support built with two square tubes and a plate.

Fig. 15 to 24 shows the placement of the combustor, turbocharger, and assembly of the components.

Figure 17: The combustor mounted to the frame using a ½ thick plate and two screws.

Figure 18: Top view of the Combustor plate

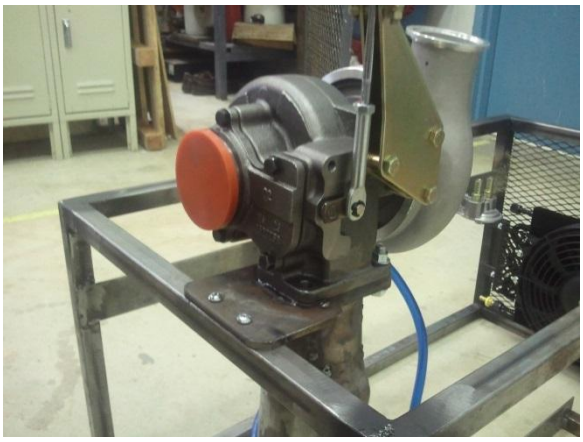

Figure 19: Combustor and turbocharger assembly

Figure 20: Frame top view

Figure 21: A square tube was added to the frame to support the weight of the combustor and turbine

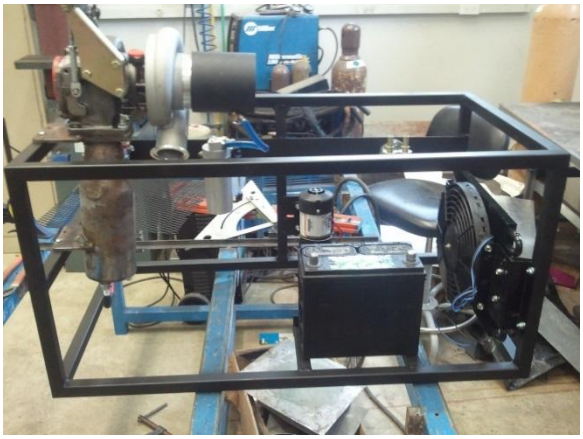

Figure 22: Painted frame

Figure 23: Oil catch can vacuum line

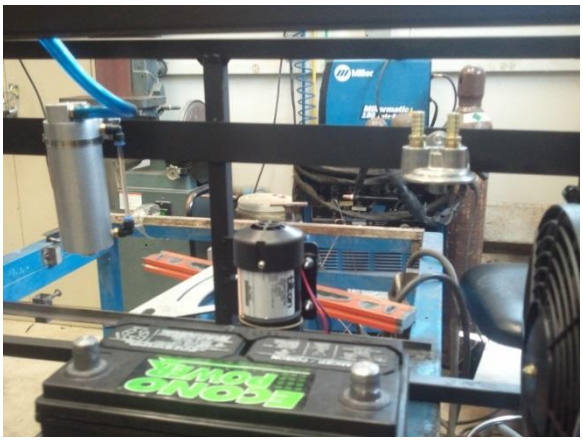

Figure 24: Assembly View

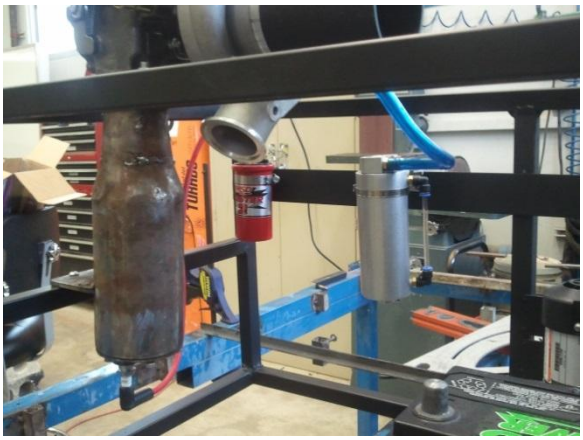

Figure 25: Ignition position

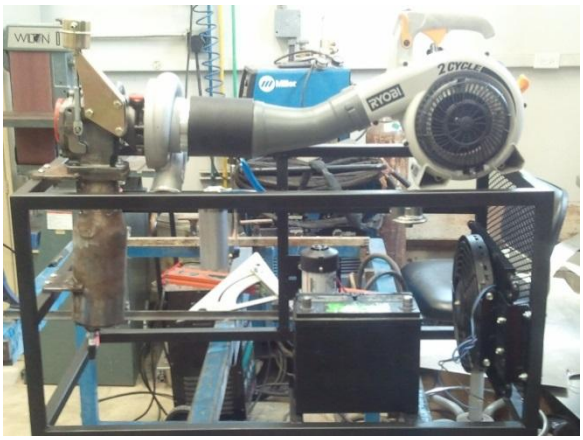

Figure 26: Front view of the frame

2.6 COMBUSTION CHAMBER: COMBUSTOR

Fig. 25 shows a schematic of the combustor. Fig. 16 presents the fabrication steps of the combustion chamber. The formulas used to dimension the combustor liner were based on the inducer diameter I (the compressor wheel diameter) that was 1.5 cm. The distance unit is in centimeter (cm).

- Combustion liner inside diameter: $A = 1.3 \times I$
- Combustion liner length: $B = 3.85 \times I$
- Combustion chamber inside diameter: $C = 2.1 \times I$
- Cross-section area of bypass section: $D = 3.6 \times I$
- Total area of combustion liner holes: $E = 4 \times I$
- Number of holes in combustion liner: $F = E \div 0.33$
- Individual size (G) of liner holes: $G = E \div F$

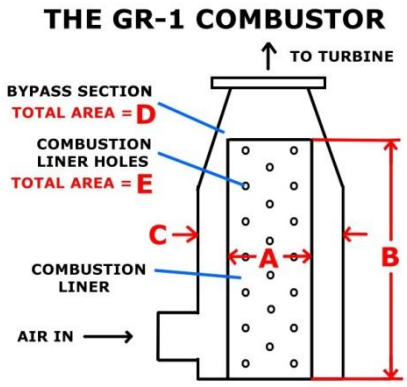

Figure 27: Combustor Schematic (RCDON)[1]

[1] Taken from http://www.rcdon.com/html/gr-1_turbojet_project_3_8_04.html

a) **b)** **c)**

Figure 28: Combustor Fabrication; a) Combustor first look, b) welding process, c) air hole

3. CONCLUSION

A gas turbine using automotive components is an economical option for research purposes. This project managed to construct a turbojet with a budget a little over $1200 during a time period of two months.

ACKNOWLEDGEMENTS

This project was supported by Summer Research Internship 2013 of the Puerto Rico Energy Center and by the Mechanical Engineering Department of Universidad del Turabo. Special thanks to Luis Tapia and Tony Santana for their support.

REFERENCES

Cengen, A. Yunus; Boles, A. Michael; Thermodynamics: an Engineering Approach 6th edition. Mc Graw Hill.

Hall LD, Mba D. (2004). Diagnosis of continuous rotor-stator rubbing in large scale turbine units using acoustic emissions. Ultrasonics, 41, pp. 765-773.

Maynard K, Trethewey M, Gill R, Resor B. (2001). Gas turbine and disk crack detection using torsional vibration monitoring: a feasibility study. Proceed. COMADEM 2001, 4-6 Sept., University of Manchester.

RCDON. Experimental Jet Engine, http://www.rcdon.com/html/gr-1_turbojet_engine_project.html, 07/20/13. (date accessed)

Authorization and Disclaimer

Authors authorize PREC to publish the paper in the internship proceedings. Neither PREC nor the editors are responsible either for the content or for the implications of what is expressed in the paper.

APPENDIX

List of Components

Figure 29: Combustion Liner. The combustion liner function is to obtain a more uniform air flow inside the combustion chamber.

Figure 30: Combustor. The combustor is where the air and the fuel are mixed and heated to produce the energy to move turbine.

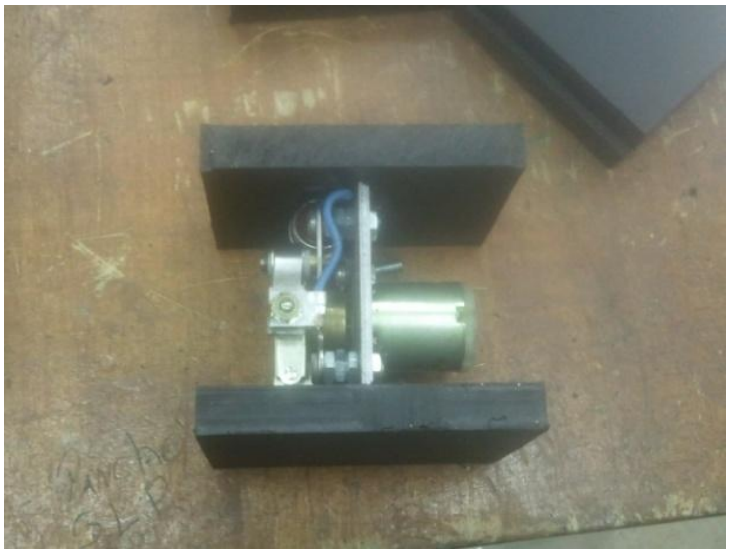

Figure 31: Ignition. The ignition function is to cause the spark to start the combustion inside the combustor.

Figure 32: Oil Pump. The oil pump is responsible of distributing the lubrication (oil) along the system.

Figure 33: Oil Can. The oil can is used to store the lubricator (oil).

Figure 34: Filter Mount. The filter is used to filter the lubricator of little particles so other part won't be affected.

Figure 35: Solenoid. The solenoid is responsible to cut the gas flow if the gas turbine needed to be shutdown.

Figure 36: Ignition Coil. The ignition coil is responsible to send the required voltage to create the spark in the ignition.

Figure 37: 12V Battery. The battery is the source of energy to power the electrical equipment of the gas turbine.

Figure 38: Gas Cylinder. The gas cylinder is the source of fuel for the system.

Figure 39: Oil Cooler. The oil cooler is used to cool down the lubricator (oil) in the system.

Figure 40: Gas Blower-Vac. The Blower is used to start up the system.

Figure 41: Gages. The gages give the pressure readings of different flow lines.

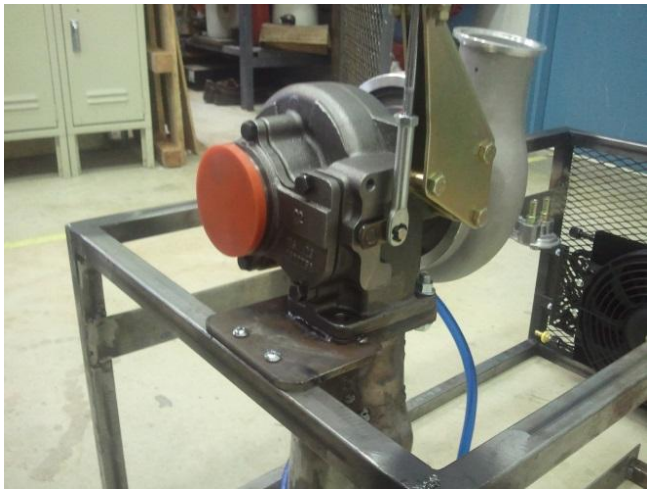

Figure 42: Turbocharger. The turbocharger is where the compressor and the turbine are located.

Figure 43: V-clamps. The V-clamps are used to secure hoses and pipes.

Figure 44: Turbo Pipe. The turbo pipe is used to connect the air hose to the turbocharger.

Kinetic analysis of the phytoremediation of fluoroquinolones using *Mimosa pudica*

Nicole Delgado
Universidad del Turabo, Gurabo, PR, n_delgado@me.com

Dennis García
Universidad del Turabo, Gurabo, PR, dgarcia-60@hotmail.com

Carlos J. Olivo
Universidad del Turabo, Gurabo, PR, olivoc1@suagm.edu

ABSTRACT

The presence of antibiotics in water and wetlands has increased significantly over the years due to the high demand of said medicine to aid the ill. This has led to their improper disposal, resulting in contamination. Ciprofloxacin and norfloxacin water, acid and basic solutions were used to study the phytoremediation capacity of *Mimosa pudica*. The maximum absorption wavelength (275.80 nm) in the UV region was determined for ciprofloxacin and norfloxacin different solutions. Two mL samples were analyzed and kinetic assays were conducted using a Schimadzu 1800 UV-Vis spectrophotometer. *M. pudica* degraded norfloxacin in water solution after 180 minutes. Ciprofloxacin's concentration was reduced after 45 minutes. With these results, more studies have to be conducted, as a clean technology appication, to remove fluoroquinolones from water bodies and wetlands in the tropical regions.

Keywords: antibiotics, fluoroquinolones, phytoremediation, water pollution

1. INTRODUCTION

Since the discovery of microorganisms and diseases in the modern era, the appearance in the antibiotics market has been a revolutionary trend to treat patients in a wide range of conditions. The increasing demand for the manufacturing of such pharmaceutical compounds has provoked another problem: presence and occurrence of antibiotics (macrolides, quinolones, etc.) in wastewaters and surface water sources that represent an environmental exposure pathway to humans, animals and agriculture. Point sources of pollution have been listed ranking from hospitals to septic tanks, livestock activities and effluents from wastewater treatment, among other not characterized sources (Focazio, et. al., 2008). The environmental occurrence and fate of several antibiotics were investigated in the aqueous phase of river water under different hydrological conditions at five sampling locations in the Seine River inner estuary in France. The target analytes belonged to different groups, including quinolones in a six-month survey where results showed that different compounds were occurring at individual concentrations reaching 544 ng/L or part per billion. Seventeen compounds were detected at least once in the survey and norfloxacin and flumequine were found to be the most ubiquitous quinolones, with detection frequencies of 33 and 75%, respectively, at the most contaminated site (Tamtam, et. al., 2008).

In a judgemental sampling assessment conducted in Puerto Rico, around 145,000 people are served with ground water sources that might be contaminated with antibiotics. A commonly prescribed quinolone type antibiotic, ciprofloxacin, for example, has been found in concentrations of 0.02 ug/L. If absorbed by plants in crops and agricultural lands, these antibiotics can pose a threat to human health and food safety (Tong, Zhuo, & Guo, 2011). In other jurisdictions of the world, the exposure and risk to public health and food safety has been assessed, primarily due to the increasing production of fluoroquinolones at the industrial level. Although contamination is

an important concern in the United States and the European Union, no regulations have been established to control the myriad of pharmaceutical compounds, antibiotics among them, which are manufactured on a big scale yearly. On the other hand, antimicrobials are the most often discussed since their presence in the environment could eventually develop resistance in pathogens (Golet, Alder, & Giger, 2002). The environmental concern with fluoroquinolones is not based in the potential of developing resistance but also in the ecotoxicity profile of these compounds, especially the hazard to food crops irrigated with antibiotics-contaminated water.

Photodegradation and adsorption of antimicrobial substances in environmental media have been documented in the literature significantly (Ge, et. al., 2010). Eighty to ninety percent of the concentration of compounds, like ciprofloxacin and norfloxacin can be removed from water using adsorption techniques (Giger, 2003). However, more studies need to be conducted on the potential of biodegradation, bioremediation and the use of local plants to detect the presence of antibiotics in soil, sediments and waters. Endemic plants are an excellent opportunity to explore phytoremediation of emerging contaminants to analyze their environmental fate and also to use them as biomarkers of the presence of contamination. *M. pudica* is an endemic plant in the tropics and grows abundantly in Puerto Rico, especially near water bodies and wetlands. Our goal is to answer the following research questions: Can *Mimosa pudica* be used as a biomarker of contamination with quinolones such as norfloxacin, ciprofloxacin, enoxacin and moxifloxacin? What are the effects of the presence of these kinds of antibiotics on a metabolic level, especially the nitrogen fixation, discharged by common people on natural waters? To what extent can *M. pudica* be used to manage this environmental problem and prevent human chronic exposure? Thus, the specific objective of this summer internship research program was to examine the phytoremediation potential of *M. pudica* in natural and agricultural waters by studying the kinetic behavior of the plant upon aqueous solutions of ciprofloxacin and norfloxacin.

Evidence has suggested that quinolones inhibit plant growth. Also, excessive use and incorrect disposition of this kind of antibiotics make it to be found in agricultural irrigation waters due to anthropological pollution of natural sources. Risk assessment protocols for antibiotics and resistant bacteria in water, based on better systems for antibiotics detection and antibiotic-resistance microbial source tracking are just starting to be discussed in the literature (Baquero, Cantón, & Martinez, 2008). Runoff water carries discharged antimicrobial substances to surface or underground deposits that may be used for irrigation in food production, resulting in an emergent food production hazard. If bio-accumulated in plants and foods, antibiotics can become a potential adverse effect in human health depending on the metabolic byproducts emerged from the biogeochemical pathway. In trace concentrations, some quinolones can cause allergic problems to consumers or even serious affections.

2. EXPERIMENTAL

The research team selected *M. pudica* to analyze its kinetic behavior in aqueous solutions of ciprofloxacin and norfloxacin, purchased from VWR. Although fluoroquinolones can be analyzed by simple and rapid high performance liquid chromatography-mass spectrometry (LC-MS) as documented by Nakata, Kannan, Jones, and Giesy (2005), the team chose spectrophotometric laboratory methods (Belal, Al-Majed, & Al-Obaid, 1999). Since quinolones and their derivatives are highly absorbing in the ultraviolet region of the electromagnetic spectrum, spectrophotometric methods have been reported to be successful in the detection of traces. Norfloxacin absorbs at 273.09nm, 277.20nm and 271.80nm in water (pH = 4), 0.1N HCl (pH = 1) and 0.1N NaOH (pH = 12), respectively, whereas ciprofloxacin absorbs at 274.27nm, 276.23nm and 271.54nm in water, 0.1N HCl and 0.1N NaOH, respectively. Spectral curves are presented on the next section. UV tests were performed using a Schimadzu 1800 spectrophotometer.

Standard solutions of ciprofloxacin and norfloxacin were prepared in water, aqueous 0.1N HCl and aqueous 0.1N NaOH in the following concentration scheme: 30, 15, 7.5, 3.75, 1.5, .75 and .5 ug/mL. The UV absorbances of these solutions were measured in the spectrophotometer in order to plot the calibration curves of each antibiotic in the different media. From the slope of these plots, graphed with MS Excel®, and following Beer-Lambert's

principle, the absorptivity coefficient constant was obtained so that the concentration of antibiotic can be calculated for the kinetic assays, once absorbances at the maximum wavelength are measured.

The kinetic analyses of the two quinolones in aqueous solutions were intended to be conducted under hydroponic conditions. *M. pudica* was to become adapted to hydroponic conditions by putting 24 specimens in contact with deionized water (final volume = 25 mL) and NPK/20:20:20 fertilizer and let adapt for one week in a controlled BIO Tronette Mark III environmental chamber at 27ºC. This adaptation could not be completed. In order to achieve the objectives of this research, specimens were freshly harvested from the university campus field and brought in to the laboratory for the tests. *M. pudica* specimens were transferred to test tubes containing 40 mL of a 30 ug/mL solution of either ciprofloxacin or norfloxacin in water, 0.1N HCl or 0.1N NaOH. Samples were taken at 15, 30, 45, 60, 120, 180, 240, 300, 360, 420 and 1440 minutes (24 hours) and UV measures were obtained with the Schimadzu 1800 spectrophotometer at the maximum wavelength of each antibiotic (275.80 nm).

Laboratory safety measures and institutional policies were followed throughout the duration of this study. Safety precautions with the use of antibiotic solutions were taken into consideration. Responsible conduct of research policies were also strictly followed in the gathering of information, performance of analyses and when reporting results.

3. RESULTS AND DISCUSSION

UV spectra for each of the 30ug/mL stock solutions of ciprofloxacin and norfloxacin were obtained in order to determine the maximum wavelength (Figure 1, 2).

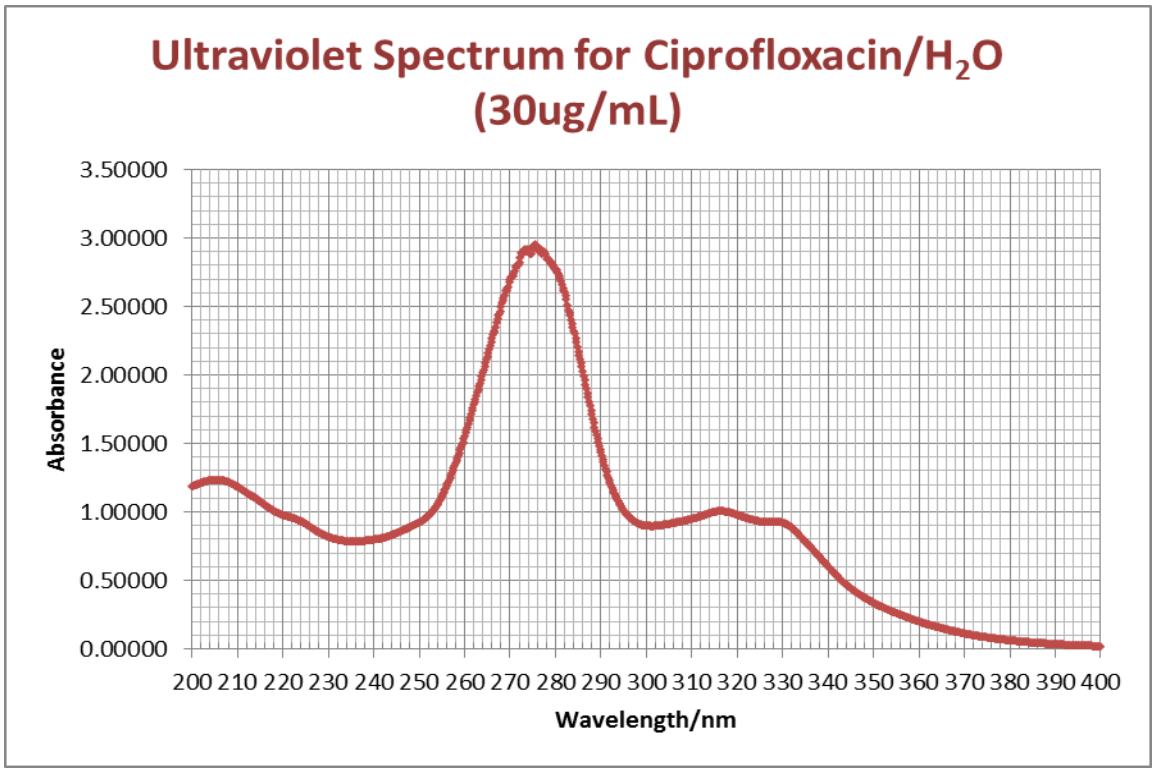

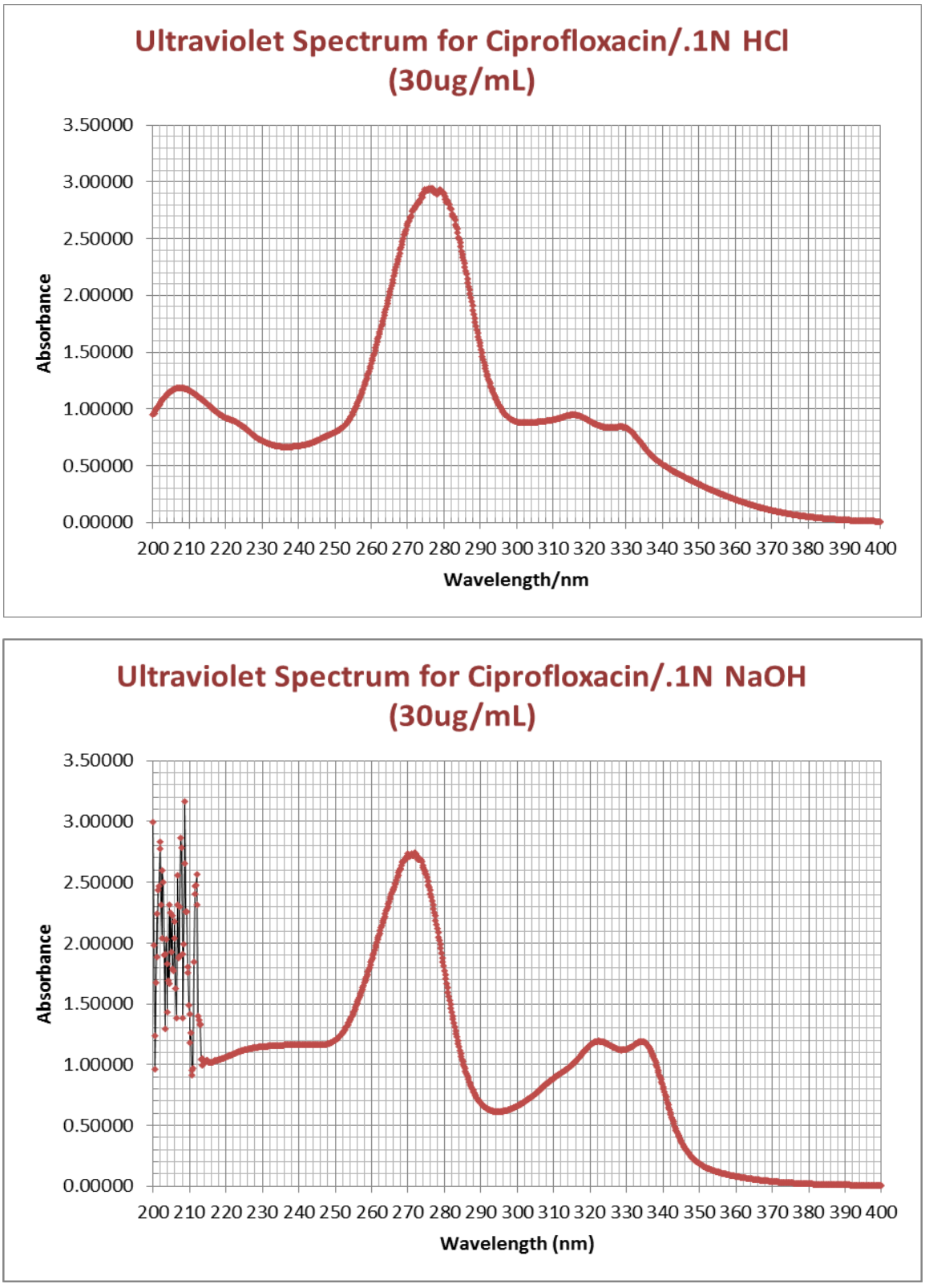

Figure 1: Spectral Curves for Ciprofloxacin

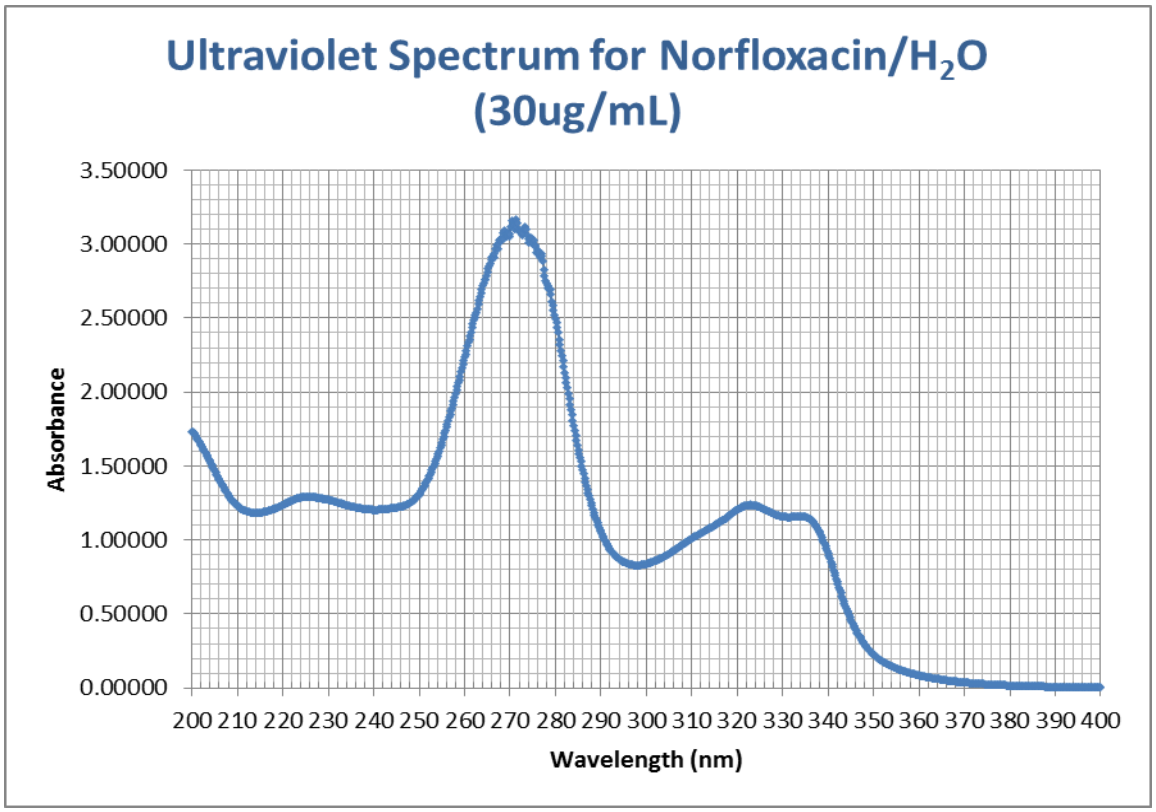
Ultraviolet Spectrum for Norfloxacin/H_2O (30ug/mL)
Absorbance
3.50000
3.00000
2.50000
2.00000
1.50000
1.00000
0.50000
0.00000
200 210 220 230 240 250 260 270 280 290 300 310 320 330 340 350 360 370 380 390 400
Wavelength (nm)

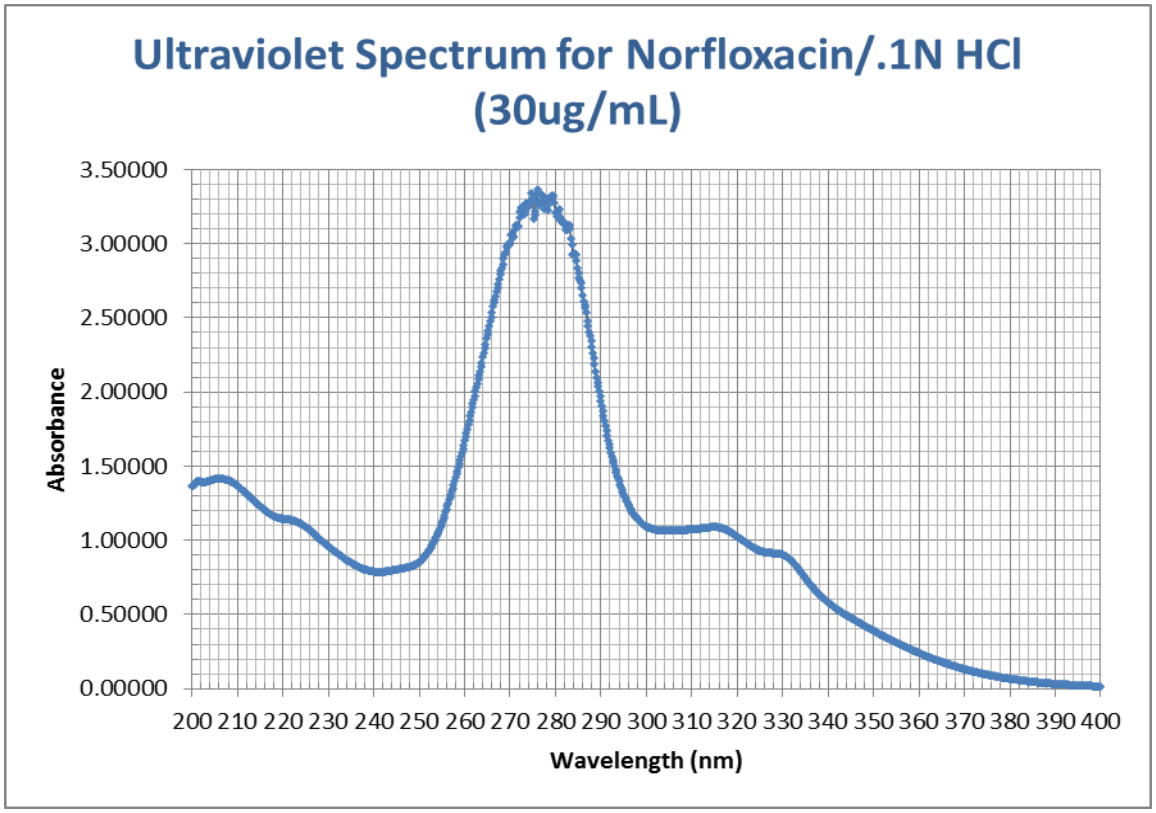
Ultraviolet Spectrum for Norfloxacin/.1N HCl (30ug/mL)
Absorbance
3.50000
3.00000
2.50000
2.00000
1.50000
1.00000
0.50000
0.00000
200 210 220 230 240 250 260 270 280 290 300 310 320 330 340 350 360 370 380 390 400
Wavelength (nm)

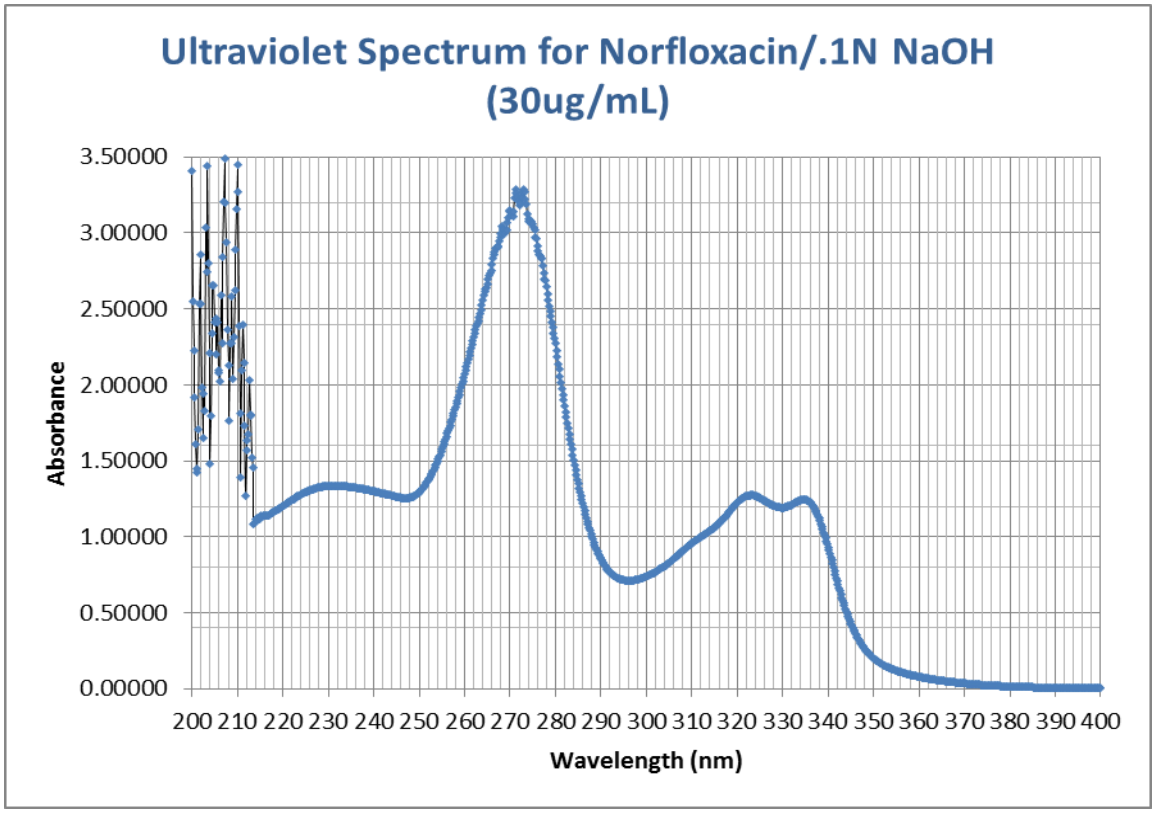

Figure 2: Spectral Curves for Norfloxacin

Calibration curves were prepared with stock solutions of 30, 15, 7.5, 3.75, 1.5, .75 and .5 ug/mL for each fluoroquinolone in water, 0.1N HCl and 0.1N NaOH. From these curves, the Beer-Lambert absorptivity constant was obtained. Results are presented on Table 1 below.

Table 1: Beer-Lambert Absorptivity Constants

Solutions	**Ciprofloxacin**	**Norfloxacin**
Water	0.0974 mL/ug	0.1095 mL/ug
0.1N HCl	0.0963 mL/ug	0.1114 mL/ug
0.1N NaOH	0.0913 mL/ug	0.1103 mL/ug

The kinetic analysis for the phytoremediation of both ciprofloxacin and norfloxacin using *M. pudica* are summarized as follows (Figure 3). Ciprofloxacin in water flows faster through the vascular system of *M. pudica* than norfloxacin. In about 45 minutes, the entire antibiotic molecules were absorbed by the specimen from the solution of ciprofloxacin in water, where the concentration reached 3.47 ug/mL, thus a reduction of 88.41% of the initial concentration was observed. On the other hand, the process lasted for about 180 minutes (3 hours) in the case of norfloxacin and the concentration reached 1.54 ug/mL or was reduced in 94.87% from the initial.

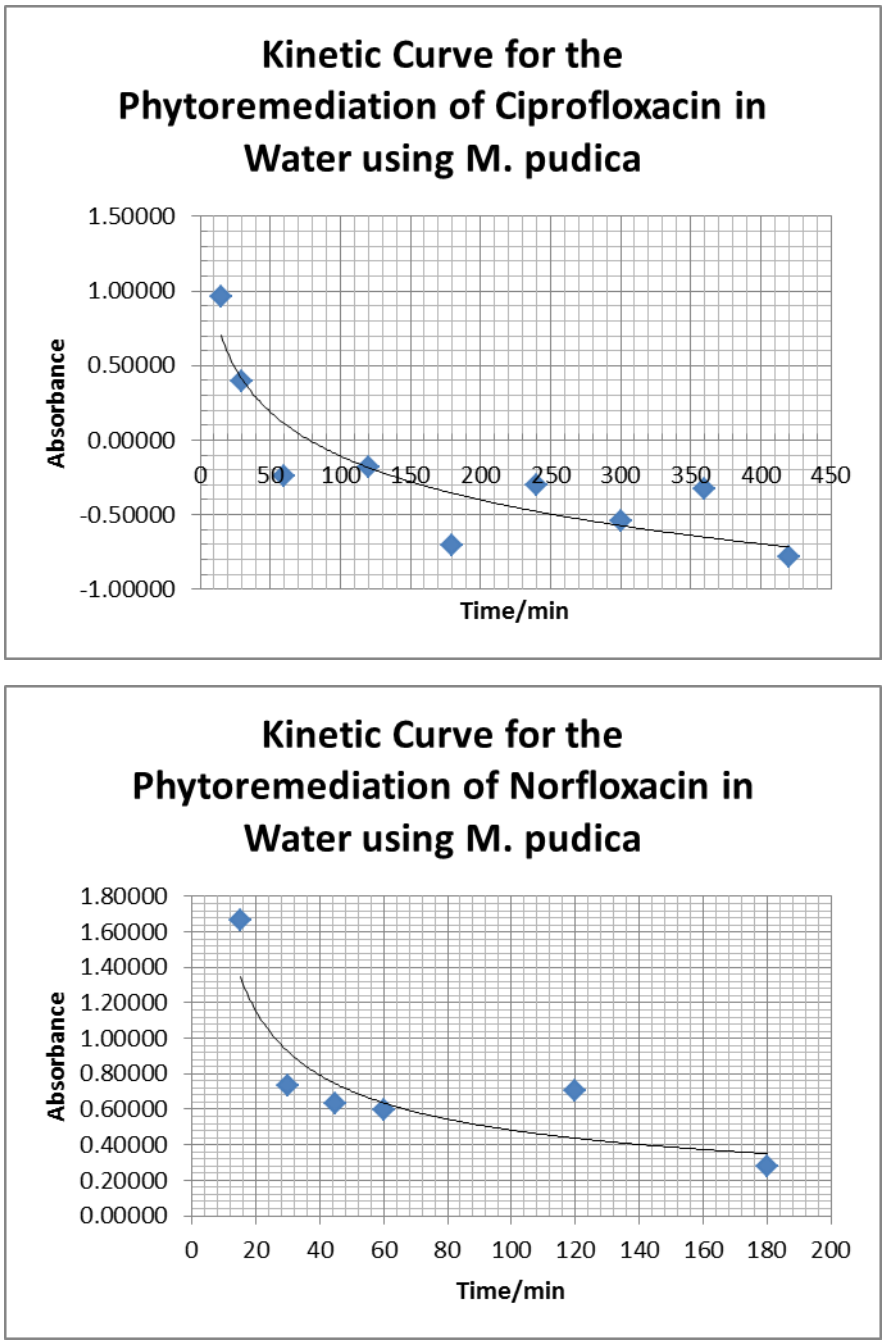

Figure 3: Kinetic Analyses

Acidic and basic solutions of both fluoroquinolones did not show the same pattern as their water solutions counterparts. In 0.1N HCl fluoroquinolones are protonated and apparently the molecules do not flow up the vascular system of *M. pudica*. The same happened in 0.1N NaOH solutions, where the fluoroquinolone molecules are deprotonated. The same results were obtained when comparing *M. pudica* assays with *Elodea canadensis* and *Lemna minor* (duckweed). More research has to be conducted to analyze the effect of temperature, pH and dissolved oxygen, among other parameters, in the phytoremediation capacity of M. pudica. Also, the type of soil where *M. pudica* could be planted can be also studied.

REFERENCES

Baquero, F.; Cantón, R.; & Martinez, JL. Antibiotics and antibiotic resistance in water environments. *Current Op Biotech* **2008**; 3:260-265.

Belal, F.; Al-Majed, AA.; & Al-Obaid, AM. Methods of analysis of 4-quinolone antibacterials. *Talanta* **1999**; 50:765-786.

Focazio, MJ.; Kolpin, DW.; Barnes, KK.; Furlong, ET.; Meyer, MT.; Zaugg, SD.; Barber, LB.; & Thurman, ME. A national reconnaissance for pharmaceuticals and other organic wastewater contaminants in the United States: Untreated drinking water sources. *Sci Total Environ* **2008**; 402:201-216.

Ge, L.; Chen, J.; Wei, X.; Zhang, S.; Qiao, X.; Cai, X.; & Xie, Q. Aquatic photochemistry of fluoroquinolone antibiotics: Kinetics, pathways, and multivariate effects of main water constituents. *Environ Sci Technol* **2010**; 44:2400-2405.

Giger, W.; Alder, AC.; Golet, EM.; Hans-Peter, E.; McArdell, CS.; Molnar, E.; Siegrist, H.; & Suter, MJF. Occurrence and fate of antibiotics as trace contaminants in wastewaters, sewage sludges and surface waters. *Intl J. Chem* **2003**; 9:485-491.

Golet, EM.; Alder, AC.; & Giger, W. Environmental exposure and risk assessment of fluoroquinolone antibacterial agents in wastewater and river water of the Glatt Valley Watershed, Switzerland. *Environ Sci Technol* **2002**; 17:3645-3651.

Nakata, H.; Kannan, K.; Jones, PD.; & Giesy, JP. Determination of floroquinolone antibiotics in wastewater effluents by liquid chromatography-mass spectrometry and fluorescence detection. *Chemosphere* **2005**; 58:759-766.

Tamtam, F.; Mercier, F.; Eurin, J.; Chevreuil, M.; & Le Bot, B. Ultra performance liquid chromatography tandem mass spectrometry performance evaluation for analysis of antibiotics in natural waters. *Anal Bioanal Chem* **2009**; 393:1709-1718.

Tamtam, F.; Mercier, F.; Le Bot, B.; Eurin, J.; Dinh, QT.; Clement, M.; & Chevreuil, M. Occurrence and fate of antibiotics in the Seine River in various hydrological conditions. *Sci Total Environ* **2008**; 1:84-95.

Tong, C.; Zhuo, X.; & Guo, Y. Ocurrence and risk assessment of four fluoroquinolone antibiotics in raw and treated sewage and in receiving waters in Hangzhou, China. *J. Agric Food Chem* **2011**; 59:7303-7309.

Ye, Z.; & Weinberg, HS. Trace analysis of trimethoprim and sulfonamide, macrolide, quinolone, and tetracycline antibiotics in chlorinated drinking water using liquid chromatography electrospray tandem mass spectrometry. *Anal Chem* **2007**; 79:1135-1144.

Authorization and Disclaimer

Authors authorize PREC to publish the paper in the internship proceedings. Neither PREC nor the editors are responsible either for the content or for the implications of what is expressed in the paper.

Optimization in Continuous Culture of *Botryococcus braunii* for the Production of Fuel Oils: Nutrient Source Assessment

Edaris Rodríguez Izquierdo
Universidad del Turabo, Gurabo, PR, USA, e_rodriguez_izqd@hotmail.com

Tanairí Cabrera Molina
Universidad del Turabo, Gurabo, PR, USA, tcm1825@gmail.com

Yomarie Bernier Casillas
Universidad del Turabo, Gurabo, PR, USA, byomarie@gmail.com

José R. Pérez Jiménez
Universidad del Turabo, Gurabo, PR, USA, ut_jperezjm@suagm.edu

ABSTRACT

The development of clean, reliable, and efficient energy conversion processes is on the most critical challenges facing the world. At the same time, the demand for energy will increase. Currently, scientist have been searching for alternative energy sources that are less harmful to the environment than fossil fuels, while reducing emissions of greenhouse gases (CO_2, SO_x, NO_x, and CH_4). Biofuel is considered a valuable clean energy alternative because decreases greenhouses gases emission in the production by sequestering CO_2 into biomass. The microalgae model produces diverse oils and rich biomass that can be fractionated for multiple applications. *Botryococcus braunii* is free-living non-toxic algae capable of producing biodiesel from diverse substrates while capturing CO_2 in its growth. Our objective is to establish optimal nutritional criteria for continuous culture of *Botryococcus braunii* for the production of fuel oils. *Botryococcus braunii* was grown in mineral media separately supplemented with nitrogen- and carbon-rich organic waste, cod and pasta cooking water respectively. Specifically, active *B. braunii* inoculum (20% final volume) was added to batch culture supplemented with various concentrations (10, 20, 30%) of organic extracts. Incubation proceeded with natural sunlight at ambient temperature. Growth was assessed by spectrophotometric measurements of optical density at 600 nm three times a day for a week. In batch culture, *B. braunii* form floating colony cluster. Higher growth was observed for in the carbon-enriched media. Ratio of oil produced will be calculated from this batch culture and continuous cultures initiated.

Keywords: *Botryococcus braunii*, optimal nutritional parameters, photobioreactor, biofuel, oil extraction

4. INTRODUCTION

The search for new sources of energy has been the subject of discussion and research for the past years. Researchers have considered the idea of seeking an alternate source much cleaner, renewable and cost effective. Previous researches have considered the use of algae, so it has been the subject of conversation at different forums (Arredondo and Vázquez-Duhalt, 1991; Sheehan *et al*, 1998; Hu *et al*, 2008). The government seeks to establish alternatives, including solar energy, wind, photovoltaic, and the use of biomass. Algae fuel or algal biofuel is an alternative to fossil fuel that uses algae as its source of natural deposits. Additionally algae don't compete for arable land and can be cultivated on fresh water, salt water and even wastewater under a wide range of temperatures, pH, and availability of nutrients. (Hernández and Vázquez, 2009). They are considered responsible for the production of 50% oxygen and 50% fixing carbon on the planet (Hernández and Vázquez, 2009). Algae have been studied for their potential in trapping carbon as well as a potential biofuel source. Cultures require water, light, CO_2, and inorganic nutrients to achieve optimal growth. The lipid, or oily part of the algae biomass can then be extracted and converted into biodiesel through a process similar to the used for any other vegetable

oil, or converted in a refinery for petroleum-based fuels.

A tiny green alga, *Botryococcus braunii* is found worldwide, but most notably in oil and coal shale deposits. It is a green, pyramid shaped planktonic microalga that is of potentially great importance in the field of biotechnology. It has gained lots of interest among the scientific community and biofuel industries due to its ability to synthesize and accumulate large amount of lipids. Many researchers had demonstrated that the biodiesel produced, using the oil extract from this microalgae is identical to biodiesel fuel (Chisti, 2007; Rosenberg *et al*, 2008). *Botryococcus braunii* also is regarded, as a potential source of renewable fuel because of its ability to produce large amounts of hydrocarbons, always depending on the strain and growth conditions, up to 75% of algal dry mass can be hydrocarbons. The oil produced can be easily converted and used for vehicle and jet fuels with more than 90% efficiency. There are more than evident reasons for which this microalga should be rather than considered as a source of energy and fuel that can lead us to advance towards a future more clean and free of many pollutants. Microorganisms such as *Botryococcus braunii* can, in the long run, reduce our dependence on fossil fuels and because of this *B. braunii* continues to attract much attention (Banerjee *et al*, 2002).

The primary focus of this research is to establish optimal criteria for continuous culture of Botryococcus *braunii* in a photobioreactor and determine optimal nutritional parameters for the production of fuel oils. Specific objectives include: (1) examine the influence of nutritional composition in oil production by *Botryococcus braunii*, (2) examine the structural response of *Botryococcus braunii* to different nutritional regimes, (3) correlating oil production (composition and quantity) with nutritional conditions, and (4) isolate and characterize native algae for the production of fuel oils.

5. METHODS

Strain and growth conditions. *Botryococcus braunni* was reactivate using an original stock from *Algae Depot*. General media for algae was prepared as recommended by provider. It consists of 1.0 L of distilled water, 2.5 g/L of sea salt, and 2 drops of F2 (nutrient solution). The nutrient solution (F2) is composed of trace metals, vitamins, and nitrogen and phosphate compounds. Previous research in our lab have shown that adding glucose to media promote the growth of the algae. An alternate media was prepared to compare algal growth with the original. This one consists of the same components but distilled water and sea salt were substitute by seawater. Three test tubes for each media was prepared with a total volume of 40 ml and sterilized for 15 minutes in an autoclave. A total of 10 µl of the stock culture of *Botryococcus braunni* was inoculate in each tube. Cultures were exposed to sunlight during the day and with artificial light during the night for about a week. Once high turbidity (dark green) was seen, 10% of each flask was inoculated in bottles with a total volume of 250 ml of media. Only the cultures that contained the original media (distilled water, sea salt, glucose and F2) were inoculated. This was done to increase the scale of algae cultivation and making it more adaptable for future work in a photo bioreactor.

Nutritional Parameters. To determine which nutritional parameters were needed to obtain optimal growth of *Botryococcus braunni* it was added different nutritional diets within the media (replacing glucose as carbon source). *B. braunni* was cultivated in media enriched with food waste such as broth extract from codfish and from pasta at different concentrations. Media was prepared as in the experimental design in test tubes at 10%, 20%, and 30% for a total volume of 6.0 ml. Several controls were prepared to maintain reliable results. They consist of media and nutritional diet for each concentration. For a period of 10 days each tube was read in a spectrophotometer to measure optical density (600 nm). This measure determined the steady growth of an organism. One measure was taken in the morning (10:00 am), at noon (1:00 pm), and in the afternoon (4:00 pm) throughout each day. In addition, other physical changes were taken into account such as, changes in color, turbidity, and particulate, among others.

Photobioreactor experimental design. The BIOSTAT® PBR 2S Photo-bioreactor was sterilized using 1L of 90% isopropyl alcohol. The unit was filled with the alcohol until all the glass tubes were covered and left 5 minutes to disinfect. The recirculation pump was started and the glass tubing was emptied. The reactor was rinsed thoroughly with sterilized water after each cleaning cycle to remove residuals of the cleaning agent from the unit.

Two liters of glucose-supplemented media was deposited aseptically into the unit and was subsequently inoculated with a 10% microalgae (*Botryococcus braunii*) concentration. Optical density measurements were taken using an optical density electrode. Light wavelength was maintained at 15 Au, and temperature was maintained at 27°C. Each of these parameters and the circulation speeds were controlled with the Micro DCU operation panel system.

6. RESULTS

Our results showed continuous growth of the algae *Botryococcus braunii* during the reactivation process. It was achieved after several trials with different media. The most appropriate media was the original media enriched with glucose. We demonstrate that glucose is an essential nutrient to stimulate algal growth and development.

Nutritional parameters results varied according to the regime and concentration applied. *Botryococcus braunii* had a preference for carbon-rich supplemented media (pasta extract) compare to the nitrogen-rich substrate (codfish broth extract). It seems that *B. braunii* preferred carbohydrates in pasta as a carbon source for energy than proteins in codfish. These results were revealed by optical density measurements. Results for pasta broth extract were higher compared to codfish.

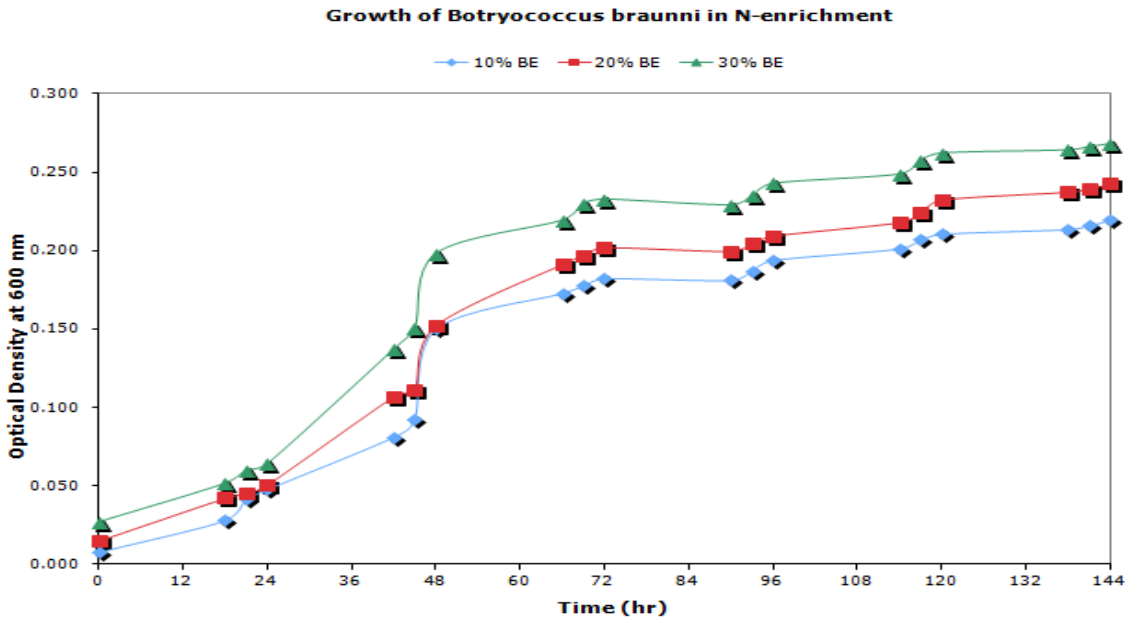

Figure 2.1. Growth of *Botryococcus braunii* under nitrogen-rich conditions (broth extract codfish).

Nutritional regime at three different concentrations (10%, 20% and 30%) revealed different level of growth, but a trend was sustained among them. At 30% concentration, both nutritional regimes resulted in greater growth. Optical density measurements were higher.

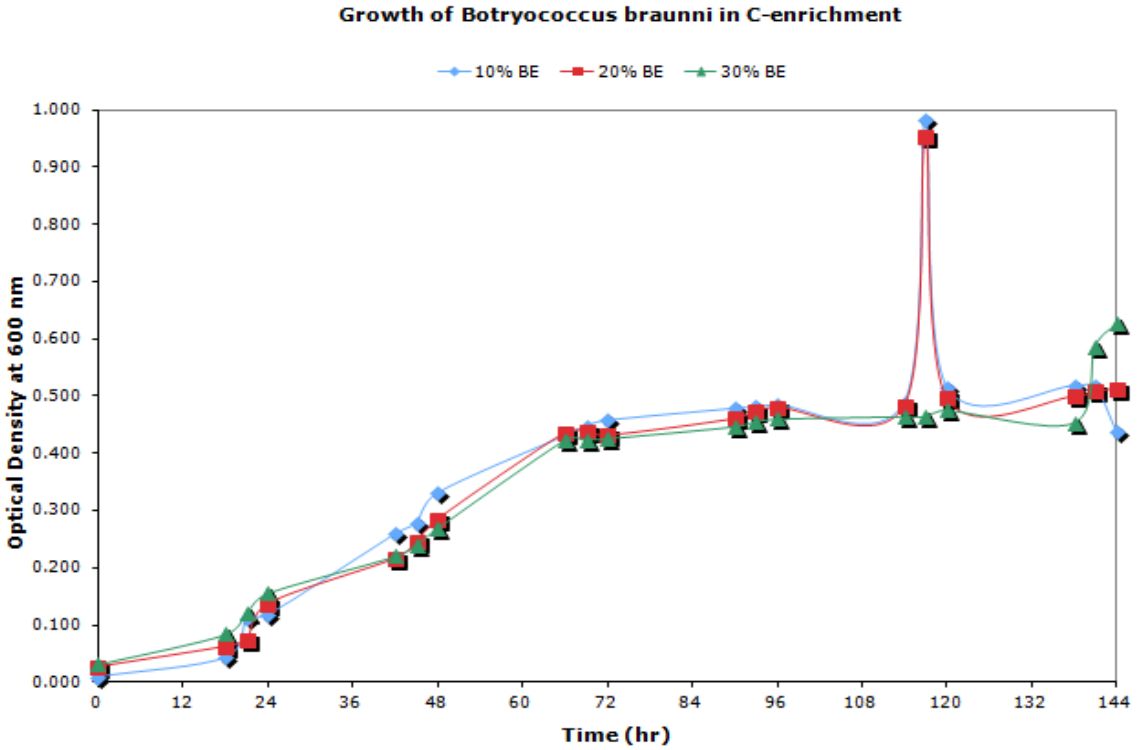

Figure 2.1. Growth of *Botryococcus braunii* under carbon-rich conditions.

Physical changes of test tubes varied greatly for both regimes. Pasta broth extracts reach a dark green color and high turbidity was observed. Whereas codfish broth extract was light green color and turbidity was not observed.

Algal cultivation in the photobioreactor achieved constant growth after for a one-week period trial.

Nutritional regime at three different concentrations (10%, 20% and 30%) revealed different level of growth, but a trend was sustained among them. At 30% concentration, both nutritional regimes resulted in greater growth. Optical density measurements were higher.

Physical changes of test tubes varied greatly for both regimes. Pasta broth extracts reach a dark green color and high turbidity was observed. Whereas codfish broth extract was light green color and turbidity was not observed.

Algal cultivation in the photobioreactor achieved constant growth after a one-week period trial.

7. DISCUSSION AND CONCLUSION

Our research results showed the possible nutritional parameters in which the algae *Botryococcus braunii* can develop and have better growth. When new nutritional parameters were established for growth optimization, it was found that these diets might affect or benefit algae growth in terms of structural composition. That is, oils for the production of biofuels as a possible source, the algae needs to be under certain physical and nutritional conditions. In our study certain nutritional diets are needed.

For the production of high quantities of oil, low levels of nitrogen and phosphorus are needed. At this level algae are exposed to drastic conditions that promotes changes in its composition. Under these circumstances, oil can be produced at high quantities and extract as a source for biofuel. Thus, oil production is associated with the source of nutrients such as nitrogen, cellulose, glycerol and other essential vitamins in metabolism for obtaining lipid concentration, which defines an optimal phycological culture.

We might think that our cultures were affected by sunlight exposure. The experiment was run for 10 days and they were exposed to sunlight for a period of 9 hours who were interrupted by several rainy days. It affected the cellular capacity of microalgae for the absorption of light from its source of energy, which is essential to its growth. With this change in exposure to sunlight, temperature was indeed affected, which is another factor that affect the optimization growth. It is essential to maintain a constant stability for optimal growing: energy source, nutrients and aeration. It would take longer to continue monitoring and investigating these great celled organism similar to terrestrial plants, for best results.

Our results have open new questions for future research and possible variants for growth optimization and oil production and used them as an energy source. Thus, future works includes the extraction of oils for biodiesel and cultivate the algae at large scales in the photo bioreactor to obtain larger quantities of oil.

8. ACKNOWLEDGMENTS

We gratefully recognize the financial support provided by the Department of Energy through the Massey Chair project at Turabo University, Summer Internship Puerto Rico Energy Center 2013, the great opportunity provided Dr. J. R. Pérez-Jiménez and the contribution of my lab mates, and colleagues in the Interdisciplinary Research Institute research. Many of the materials and instruments used were provided by *NSF-ATE PRIMER Tropical Bioprospecting Venture at CETA* (DUE-0903274) and *PRIMER Bioprospecting for Bioenergy* (US Forest Service 11-DG-11330101-111) to Dr. Pérez-Jiménez. Without the support and help of all these resources could not carry out such work.

CITATIONS AND REFERENCE SECTION

Abd El-Moneim M. R. Afify, EA Shalaby, SMM Shanab. (2010). Enhancement of biodiesel production from different species of algae. *Grasas y Aceites.* 61: 416-422.

Apt KE, PW Behrens. (1999). Commercial developments in microalgal biotechnology. J Phycol. 35:215-226.

Barbosa MJ, J Hoogakker, RH Wijffels. (2003). Optimisation of cultivation parameters in photobioreactors for microalgae cultivation using the A-stat technique. Biomol Eng. 20:115-123.

Belotti, Scarsella, G. Filippis, and Bravi M. "Study on the optimal growing conditions of Chlorella vulgaris in bubble column photobioreactors." Dept. of Chemical Engineering Materials Environment. N.p., 2010. Web. 7 Aug 2012. <http://www.aidic.it/ibic2010/webpapers/58Scarsella.pdf>.

Bojan Tamburic BT. 2008 Parameters Affecting the growth and hydrogen of the Green Alage *Chlamydomonas reinhardtii*. Energy resources (biofuels). Faculty of Engineering Imperial College London, London SW7 2AZ, UK (13-54), pp.96

Chisti Y. 2007. Biodiesel from microalgae. Biotechnol Adv. 25:294–306.

Dalrymple OK, Halfhide T, Udom I, Gilles B, Wolan J, Zhang Q, Ergas S. (2013). Wastewater use in algae production for generation of renewable resources: a review and preliminary results. Aquat Biosyst. Dec 4. PubMed PMID: 23289706.

Feng Y, C Li, D Zhang. (2011). Lipid production of *Chlorella vulgaris* cultured in artificial wastewater medium. Bioresource Technology. 102:101

Gaurav K, R Srivastava, R Singh. (2012). Exploring Biodiesel: Chemistry, Biochemistry and Microalgal source. International Journal of Green Energy. 120910085609008

Gomes de Oliveira Dal'Molin G, L-E Quek, RW Palfreyman, LK Nielsen. (2011). AlgaGEM – a genome-scale metabolic reconstruction of algae based on the *Chlamydomonas reinhardtii* genome. BMC Genomics. 12:S5

Harwood JL, IA Guschina. (2009). The versatility of algae and their lipid metabolism. Biochimie. 91:679

Hernandez, A., & Vazquez, R. (2009). Biodiesel a partir de microalgas. BioTecnología. 13:38-61.

Hossain ABM, Salleh A. 2008. Biodiesel fuel production from algae as renewable energy. Am. J. Biochem. and Biotechn. 4:250-254

Kaplan D, Cohen Z, Abeliovich A. (1986). Optimal Growth Conditions for *Isochrysis galbana*. *Biomass*. 9:37-48

Kim HW, Vannela R, Rittmann BE. (2013). Responses of *Synechocystis* sp. PCC 6803 to total dissolved solids in long-term continuous operation of a photobioreactor. Bioresour Technol. 128:378-84. PubMed PMID: 23201518.

Liu J, Sommerfeld M, Hu Q. (2013). Screening and characterization of *Isochrysis* strains and optimization of culture conditions for docosahexaenoic acid production. Appl Microbiol Biotechnol. 8:e52382. PubMed PMID [Epub ahead of print]: 23423326.

Luque R and JA Melero. (2011). Advances in biodiesel production: processes and technologies. Woodhead Pub Ltd. Oxford ; Philadelphia. 288 p.

Ogbonna JC, Tanaka H. (2000). Light requirement and photosynthetic cell cultivation-development of processes for efficient light utilization in photobioreactors. J Applied Phycol. 12:207-218.

Olaizola M. (2003). Commercial development of microalgal biotechnology: From the test tube to the marketplace. Biomol. Eng, 20: 459-466.

Oncel SS and O Akpolat. (2006). An integrated photobioreactor system for the production of *Spirulina platensis*. Biotechnology. 5:365-372.

Pulz O. (2001). Photobioreactors: Production systems for phototrophic microorganisms. Applied Microbiol Biotechnol. 57:287-293.

Quintana N, F Kooy, MD Rhee, GP Voshol, R Verpoorte. (2011). Renewable energy from Cyanobacteria: energy production optimization by metabolic pathway engineering. Applied Microbiology and Biotechnology. 91*:*471

Singh A, PS Nigam, JD Murphy. (2011). Renewable fuels from algae: An answer to debatable land based fuels. Bioresource Technology. 102*:*10

Starr, R. C. and Zeikus, J. A. (1993), UTEX—The culture collection of algae at the University of TEXAS at Austin 1993 List of Cultures. Journal of Phycology, 29: 1–106.

Subramaniam R, S Dufreche, M Zappi, R Bajpai. (2010). Microbial lipids from renewable resources: production and characterization. Journal of Industrial Microbiology & Biotechnology. 37*:*1271

Tanaka, H, JC Ogbonna, H Yada. (1995). Effect of cell movement by random mixing between the surface and bottom of photobioreactors on algal productivity. J Ferment Bioeng. 79:152-157.

Authorization and Disclaimer

Authors authorize PREC to publish the paper in the conference proceedings. Neither PREC nor the editors are responsible either for the content or for the implications of what is expressed in the paper.

Penstock Dimensions Optimization Software for Low Head Hydroelectric Plants

Alan López García
University of Puerto Rico at Mayagüez, Mayagüez, Puerto Rico, alan.lopez1@upr.edu

Ricardo Esbri Amador, PE, PA
Consulting Engineer, Caguas, Puerto Rico, esbri@hotmail.com

ABSTRACT

Financialy focused evaluation is a key aspect in low head hydroelectric projects. Even though technology has advanced to the point of making it economically viable to obtain electricity with a low difference in height, optimizing the penstock dimensions to obtain a maximun energy output is still a crucial task. Given the nature of hydroelectric plants each new design in a different location needs specific, time consuming, optimization calculations that vary at the same rate as the cost of their potential materials. We have programed a tool that computes the optimization of the penstock's dimensions speeding up the project design and standarizing the optimization process.

Keywords: penstock, dimensions, optimization, software, diameter

1. INTRODUCTION

Optimal penstock design is a "crucial part of [a] water power electrical structure"(Purwati and Wahyun, 2010). Penstock optimization takes into consideration project specifics like the average flow, the head, the specific viscosity and density of the liquid, and the selected turbine efficiency while also observing financial aspects like the specific weight of the material, installation cost, and the project funding interest rate. Given the nature of constant chage of the financial aspects for the project, "[t]his dynamic forces the engineer to be more diligent in terms of economic penstock sizing, to apply material cost and value of energy parameters in the best possible manner"(American Society of Civil Engineers, 2012). Having considered this we can say that optimization calculations are specific to each project at a given moment, requiring the engineer to spend a vast amount of time in this task.

In this paper we go through the specifics on the development of a program that computes and gives the output of the optimum dimensions for a specific penstock design given the Economic Diameter considerations on steel penstocks worked by the American Society of Civil Engineers, adapted with the Darcy-Weisbach, Colebrook, and Curchill's equations on friction and headloss inside pipes as worked on and explained by Hodges and Taylor(1989).

2. MATHEMATICAL BACKGROUND

The American Society of Civil Engineers(2012) suggests a series of equations to optimize the dimensions of steel penstocks with a predetermined friction coefficient. We adapted the equations adding the calculation of specific friction and headloss for each computation, adapting thus the equations to be used with different materials and making our optimization more flexible and precise.

2.1 HEADLOSS

The dissipated energy inside a pipe due to friction through the pipe caused by the pipe wall skin is known by definition as major headloss (Hodges and Taylor, 1989). Headloss is key to calculating the optimal dimensions of penstock beacause "headloss is directly proportional to pipe length… [and it] is proportional to pipe diameter"

(Hodges and Taylor, 1989). We used the Darcy-Weisbach equation for headloss provided by Hodges and Taylor (1989):

2.1.1 DARCY-WEISBACH HEADLOSS EQUATION

$$h_f = f_{D\text{-}W}\frac{L}{D}\frac{V^2}{2g}$$

Where L stands for the length of the pipe, D the diameter, V the average fluid velocity, g the gravitational acceleration and $f_{D\text{-}W}$ the friction factor.

2.2 FRICTION FACTOR

The friction factor is a dimensionless coefficient and can be defined as a complex function in the form:

$$f = f(Re_D, \frac{\varepsilon}{D})$$

"where Re_D is the Reynolds number based upon the pipe diameter and $\frac{\varepsilon}{D}$ is the relative roughness of the pipe"(Hodges and Taylor, 1989).

2.2.1 IMPLICIT EQUATION OF COLEBROOK

$$\frac{1}{\sqrt{f}} = \log\left(\frac{\varepsilon}{3.7D} + \frac{2.51}{Re_D\sqrt{f}}\right)^{-2}$$

The implicit equation of Colebrook was selected because it "has been accepted as the most accurate functional representation of the Moody diagram in the turbulent zone" (Hodges and Taylor, 1989).

2.2.2 LAMINAR FLOW FRICTION FACTOR

$$f = \frac{64.0}{Re_D}$$

2.2.3 CHURCHILL EQUATION

The Churchill equation selected as a first approximation of the friction factor because it is designed to work with both turbulent and laminar flow giving a good estimate. This equation states:

$$f = 8\left[\left(\frac{8}{Re_D}\right)^{12} + \frac{1}{(A+B)^{1.5}}\right]^{\frac{1}{12}} \text{ where}$$

$$A = \left\{2.457 \text{ LN}\left[\frac{1}{\left(\frac{7}{Re_D}\right)^{0.9} + \left(\frac{0.27\varepsilon}{D}\right)}\right]\right\}^{16} \text{ and}$$

$$B = \left(\frac{37{,}530}{Re_D}\right)^{16}$$

2.3 REYNOLDS NUMBER

The Reynolds Number is defined as:

$$Re_D = \frac{\rho V D}{\mu}$$

where ρ stands for the density of the fluid and μ for its dynamic viscosity.

2.4 INSTALLATION COST

The capital cost of the penstock is calculated with the equations from the American Society of Civil Engineers(2012):

$$U = \pi WCtD$$

where W is the specific weight of steel(lb/ft^3), C the installation cost of penstock ($/lb), t the shell thickness, and D the pipe diameter. The thickness is calculated by:

$$t = \frac{FHD}{2S}$$

Where F stands for the conversion factor between ft of water to lb/in^2, H is the weighted average of the design head (ft), and S is the maximum allowable stress (lb/in^2).

2.5 POWER REVENUE LOSS

The annual power revenue loss (kw/year) is calculated with the equation recommended by the American Society of Civil Engineers:

$$PRL = \frac{0.002129fEQ^3}{D^5}$$

where E is the overall turbine/generator efficiency, and Q the design flow (ft^3/s). Multiplying the PRL by a present worth factor we obtain the present worth of the power revenue loss.

2.6 ECONOMIC DIAMETER

The Economic Diameter is calculated using the American Society of Civil Engineers(2012) equation:

$$D = 0.5\left[\frac{SfgMEQ^3(pwf)}{WCH}\right]^{0.1429}$$

where M is the composite value of power ($/kWh), (pwf) the present worth factor with a specified interest rate and repayment time, C the capital cost of penstock installed, W the specific weight of material used, h the hours of operation, H the design head and f the calculated friction factor.

3. OPTIMIZATION

By analyzing the selected equations we can observe that the Economic Diameter Function is dependent of a stated pipe diameter (figure 1). Because we are dealing with the same penstock diameter throughout the pipe, the optimized diameter is defined by derived implicit equation in which the Economic Diameter must be equal to the pipe diameter used to compute the Reynolds number. We approached this mathematical equivalence with an Object Oriented Programming approach to iterative optimization. Object Oriented programming was selected because of the black-box characteristics of the depending equations. We arbitrarily assigned the value of one foot (1ft.) to the first diameter iteration.

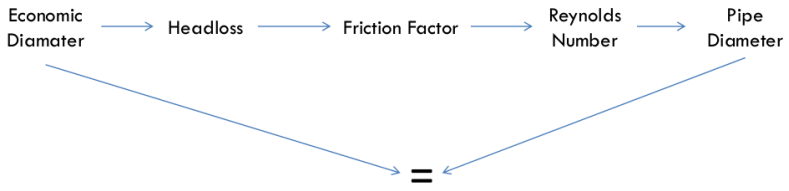

Figure 1: Diameter Equation Dependencies

4. COMPUTER PROGRAM

A first prototype of a computer program was developed to compute the optimized penstock dimensions. The optimization approach design can be appreciated by the following flowchart:

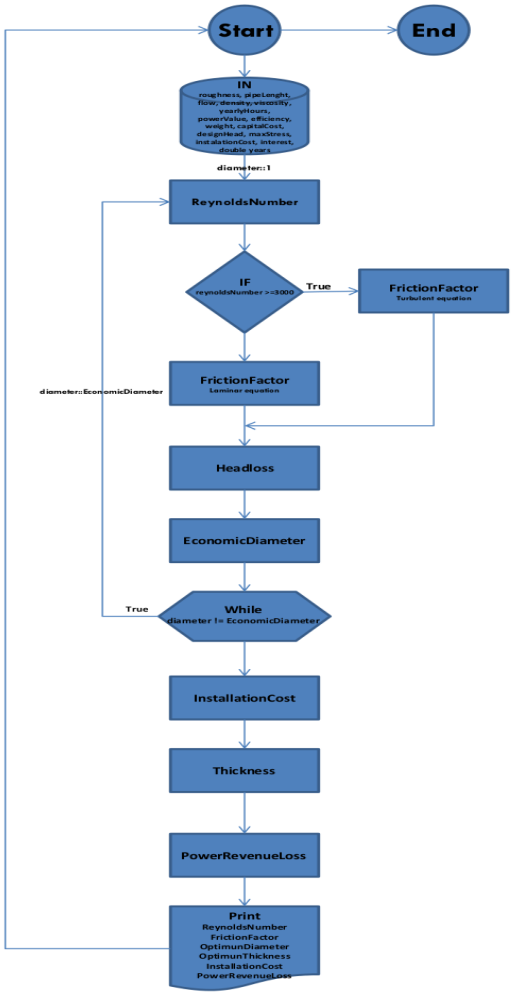

Figure 2: Optimization Flowchart

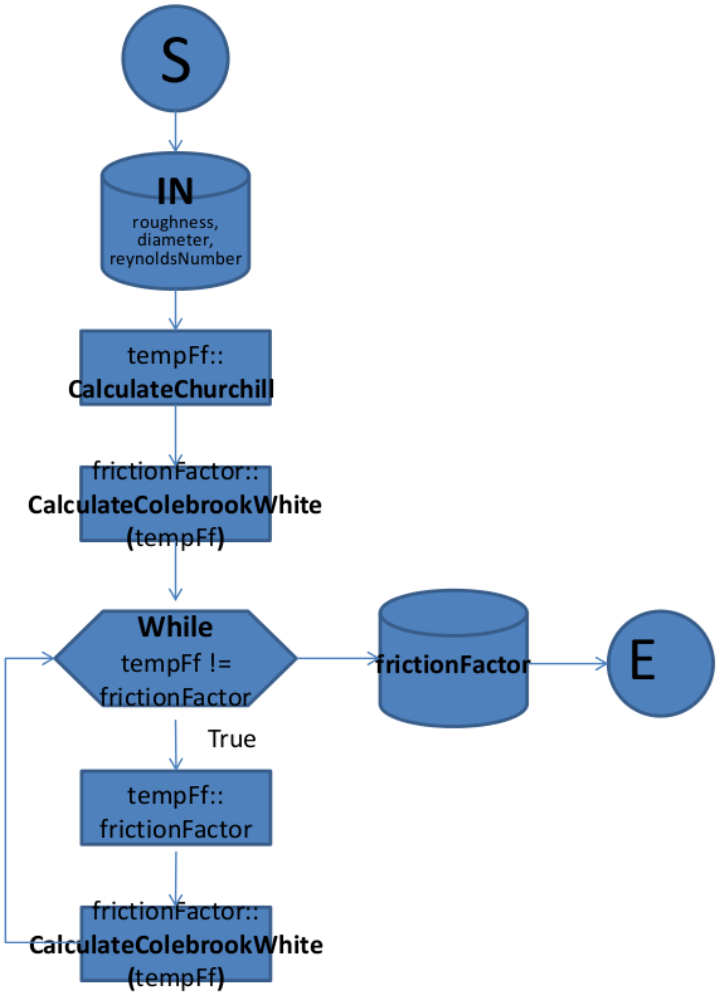

Figure 3: Turbulent Flow Friction Factor Flowchart

The program takes as inputs:

- Pipe Roughness(ft)
- Pipe Flow (ft^3/s)
- Pipe Length (ft)
- Fluid Density (slugs/ft)
- Fluid Viscosity ($lb*s/ft^2$)
- Annual Hours of Operation (h)
- Composite Value of Power ($/kW*h)
- Turbine/generator Efficiency
- Specific Weight of pipe (lb/ ft^3)
- Capital Cost of Penstock Installed ($/lb)
- Design Head (ft)
- Allowable Stress (lb/in^2)
- Installation Cost ($/lb)
- Interest Rate
- Repayment Perios (years)

The program gives as outputs:

- Reynolds Number
- Friction Factoe
- Headloss (ft)
- Optimun Diameter (ft)
- Optimun Thickness (ft)
- Installation Cost ($)
- Power Revenue Loss (kW/year)
- Power Revenue Loss Present Worth ($)

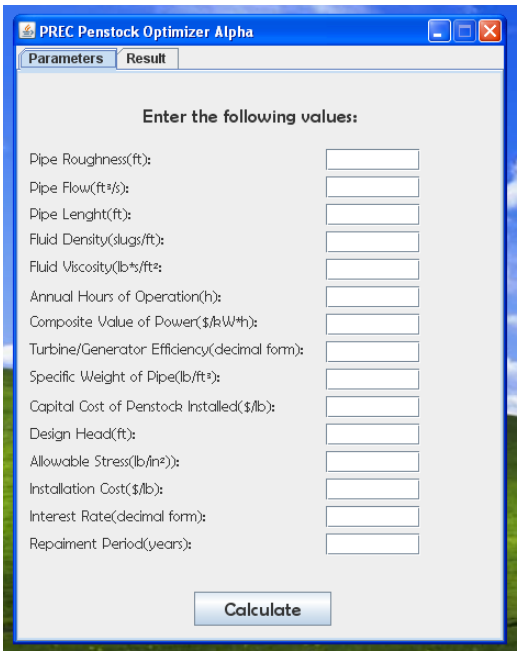

Figure 4: PREC Penstock Optimizer Alpha Main Window

5. TEST RUN RESULTS

We compared the results of the optimized diameter obtained by our program with the by hand calculations of a pressure governs penstock calculated by hand and used as an example in the American Society of Civil Engineers *Steel Penstocks* manual. For the Reynolds number calculation we used the standard 0.00015(ft) as the pipe roughness of Steel. The data entered:

- Pipe Roughness(ft): 0.00015
- Pipe Flow (ft^3/s): 2900
- Pipe Length (ft): 500
- Fluid Density (slugs/ft): 1.94
- Fluid Viscosity ($lb*s/ft^2$): 0.0002715
- Annual Hours of Operation (h): 7075
- Composite Value of Power ($/kW*h): 0.05
- Turbine/generator Efficiency: 0.85
- Specific Weight of pipe (lb/ ft^3): 490
- Capital Cost of Penstock Installed ($/lb): 3.5
- Design Head (ft): 442.4

- Allowable Stress (lb/in^2): 20000
- Installation Cost ($/lb): 1
- Interest Rate: 0.0875
- Repayment Perios (years): 50

We obtained an Economic Diameter of 15.243 (ft) versus 15.00(ft) of the example

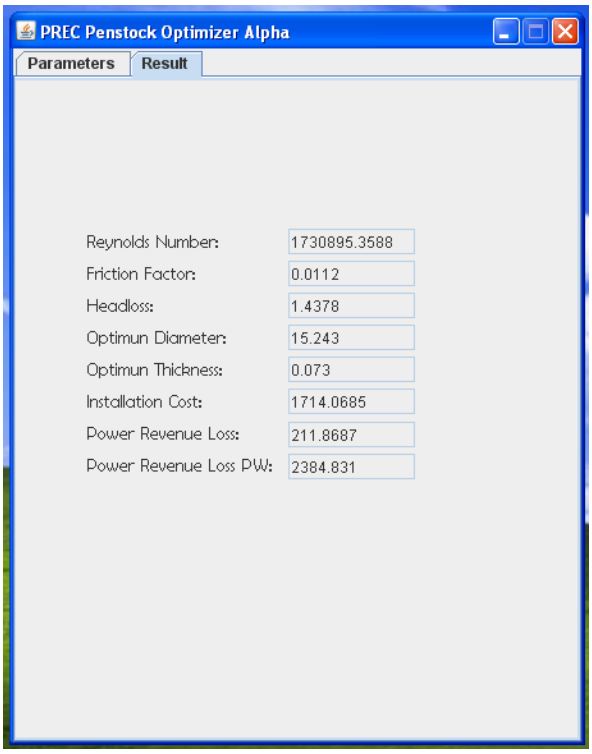

Figure 5: PREC Penstock Optimizer Alpha Test Results Window

6. CONCLUSION

The percentage of difference between our programs optimization and the American Society for Civil Engineer's Manual (2012) is of 1.59%. This small percentage of difference is due because in our optimization we continuously calculate the specific Reynolds number, friction factor, and headloss until finding the optimum diameter. We understand that this modification of the equations makes our program faster and more accurate than calculating the example by hand.

We also ran the program with values bigger and smaller than the expected optimized diameter for the value of the diameter in the first iteration. Our program always printed the same expected output proving the precision of the designed algorithm.

7. FUTURE WORK

We plan to continue implementing this tool to its full potential in several areas. Even though a minor headloss class was programed, by the submission of this paper it has not been implemented to be used in the optimization. Also adding back and forth SI unit capability to the program is contemplated for the near future.

Once fully operational the program and source code will be released under a Creative Commons license.

REFERENCES

American Society of Civil Engineers. (2012). *Steel Penstocks: ASCE Manuals and Reports on Engineering Practice No. 79*, 2nd edition, American Society of Civil Engineers, Virginia, USA.

Baños, R., et al. (2011). "Optimization methods applied to renewable and sustainable energy: A review". *Renewable and Sustainable Energy Reviews*, Vol. 15, Issue 4, pp 1753-1766.

Hodges, B. K., and Taylor R.P. (1989). *Analysis and Design of Energy Systems*, 2nd edition, Prientice Hall, USA.

Purwati, E., and Wahyun, H.I. (2010). "Optimization on Penstock Dimension of Ampel Gading Hydro Electrical Power, Indonesia". *International Journal of Academic Research*, Vol. 2, Issue 6, p 307.

Authorization and Disclaimer

Authors authorize PREC to publish the paper in the internship proceedings. Neither PREC nor the editors are responsible either for the content or for the implications of what is expressed in the paper.

Photocatalytic degradation of the UV-filter p-aminobenzoic acid with TiO_2 nanowires

Tracey Rodríguez Franqui
Universidad del Turabo, Gurabo PR. tracey-064@hotmail.com

Euvelisse N. Jusino Del Valle
University of Puerto Rico, San Juan PR. e.n.jusino@gmail.com

Loraine M. Soto-Vázquez
Universidad del Turabo, Gurabo PR. lorainesoto@gmail.com

Francisco Márquez Linares
Universidad del Turabo, Gurabo PR. fmarquez@suagm.edu

ABSTRACT

With climatic change, new challenges in water treatments are emerging concern in water management. The presence of emerging pollutants such as pharmaceuticals and personal care products (PPCPs) is alarming to the water purifying systems. One of the PPCPs used seasonwise are the variety of sunscreens avalilable to public, which is bioacumulating in our waters due to its non-degrading and UV-absorbant feature. In this project we studied the photocatalytic degradation of a sunscreen active ingredient, p-aminobenzoic acid (PABA). We succesfully synthesized and characterized, by SEM-EDS, TiO_2 nanowires in order to use them as catalyst for the photodegradation of PABA. The photodegradation was studied by varying the catalyst loading while monitoring the photoreaction with UV-Visible Spectra and Fluorescence. As a result, 0.6 g/L TiO_2 was found to be the optimal catalyst loading.

Keywords: nanowires, degradation, p-aminobenzoic acid, green chemistry

1. INTRODUCTION

With climatic change, new challenges in water treatments are emerging concern in water management. The presence of emerging contaminants in these waters is a potential major problem in our environment. These pollutants are a large relatively new group of unregulated compounds such as pharmaceuticals personal care products (PPCPs), plasticizers, surfactants, and herbicides whose ecotoxicological effects are relatively unknown. In order to remove these emerging contaminants from our water source, water systems have been developed to efficiently eliminate these pollutants (Deng 2009). Sunscreens are one of the PPCPs with an incresing consumption due to the concern and scientific interest of the development of dangerous skin illness such as cancer (Zhang et al. 2010) However, sunscreens also have been detected in surface waters (e.g. lakes and rivers), wastewaters, drinking water, soil sludge and fish. These sunscreens are generally more lipophilic than traditionally regulated pollutants and therefore have a bioaccumulation potential (Díaz-Cruz , Poiger et al. 2004, Balmer et al. 2005, Plagellat et al. 2006, Buser et al. 2006). One of the major concerns regarding sunscreen products is p-aminobenzoic acid (PABA) which was one of the first active ingredients to be used in sunscreen in concentrations up to 5% (Osgood et al. 1982) The water resistance of typical sunscreens is very low, retaining only 10-30% of the cream on the skin after one immersion in water (Lambropoulou et al. 2002). This indicates that a great amount of PABA is being released in our water source for each consumer.

Science has evolved in order to find new methods to retrieve or degrade hazardous compounds from our water sources. However, not all procedures for water cleansing are ecofriendly. The "greener" environmentally friendly processes in chemistry and chemical tehnology are becoming increasingly popular and are much needed as a result of worldwide problems associated with environmental contamination (Kharissova et al. 2013). The 12 principles of green chemistry have now become a classic guide for chemists and chemical technologists worldwide in developing less hazardous chemical syntheses and responses to water pollution (Anastas and Warner 1998). Within the last decade, green chemistry has been recognized as a potenial approach toward scientifically based environmental protecion. Recently, photocatalysis has come to be considered one of the most important environmentally friendly, clean chemical technologies for green chemistry (Anastas et al. 2000).

Photocatalysis is a potential technology for the decomposition of organic pollutants in wastewaters, such as benzene and its derivatives, which have a significant potential hazard to human health and to the environment (Centi and Perathoner 2003, Hutchings 2007). Photocatalytic processes involving the oxidation of organic compounds in wastewater are achieved by the reactive hydroxyl radical. Titatium dioxide (TiO_2) is a natural ocurring oxide of titanium. In nature, it exists in five forms, i.e. rutile, anatase, brookite, monoclinic and orthorombic (Min and Rahman 2011). TiO_2 is well known for its widespread application in paints, sunscreens, environmental treatment and purification purposes (Auvinen and Wirtanen 2008, Carlotti et al. 2009, Liao and Que 2010, Mohamed and Mkhalid 2010). Photocatalytic reaction is initiated with the enough input of radiation, equal or higher than the band-gap energy of the target semiconductor which cause a molecular excitation and charge separation. As a result, mobile eletrons-holes pairs will be generated and migrate to the surface of the semiconducror to take part in the photocatalytic reaction (Chun et al. 2000). A photocatalytic reaction in the presence of hydrogen peroxide increases the concentration of hydroxyl radicals in the solution, thereby enhancing the rate of photocatalytic oxidation (King Saud Univerity, 2012).

$$TiO_2 + hv\ (<387\ nm) \rightarrow e_{CB}^- + h_{VB}^+ \quad [1]$$

$$h_{VB}^+ + (PABA) \rightarrow \text{Intermediates} \rightarrow CO_2 + H_2O \quad [2]$$

$$H_2O + h_{VB}^+ \rightarrow \square OH + H^+ \quad [3]$$

$$\square OH + PABA \rightarrow \text{Intermediates} \rightarrow CO_2 + H_2O \quad [4]$$

The photocatalytic and hydrophylic properties of TiO_2 makes it close to an ideal catalyst due to its high reactivity, reduced toxicity, chemical stability and lower costs (Fujishima et al. 2000). Greener synthesis of nanowires provides advancement over other methods as it is simple, cost effective and relatively reproducible and often result in more stable materials. Heterogenous photocatlysis process utilizes the solar energy and has been proven to be an efficient technique for the elimination of pollutants from aqueous and gaseus media (Hoffman et al. 1995).

For this project our intent was to synthesize TiO_2 nanowires in order to employ them as catalyst for the photocatalytic degradation of PABA in water. Hence, an analysis of optimum catalyst loading to achive the best degradation of PABA in UV-VIS spectroscopy was used and also fluorimeter for monitoring the reaction process.

2. REAGENTS AND MATERIALS

ACROS-Organics® Ethyl Alcohol; SIGMA-ALDRICH® 2-Propanol (99.9%); SIGMA-ALDRICH® Acetone (99.9%); Fischer $TiCl_4$; ACROS-Organics® HCl (37%); Fisher Scientific® H_2O_2 (50%); SIGMA-ALDRICH ACS reagent NaOH, P-Aminobenzoic Acid/ Autoclaves, General Electric® Hg Lamps (2/120V-Visible Spectra), Stirring plate, UV-Spectrophotometer, Fluorimeter, StarnaCells-Quartz Spectrophotometer cells (1mm) SEYAN ELECTRONICS-Silica substrates; GELMAN GHP-0.45µm; METTLER TOLEDO pH meter. All the reagents were used as is.

3. METHODOLOGY

Synthesis of TiO_2 nanowires

The Silica substrates were thoroughly cleansed by ultrasonicating with 30.0 mL of Acetone, 2-Propanol and Deionized H_2O for 10 minutes each respectively. A 1:1 solution of HCl 35% and deionized water was stirred for 10 minutes. After, (3.50 $\pm$ 0.05) mL of $TiCl_4$ was added dropwise and stirred for an additional 10 minutes. This solution was added in the autoclaves in contact with the substrates. Finally the autoclaves were placed in an oven at 180 °C during 2 hours. The catalyst were then rinsed with deionized water and dried at 60 °C overnight and stored for characterization and further experiments.

Characterization of TiO_2 Nanowires

For the characterization of the Titanium dioxide nanowires, Scanning Electron Microscope (SEM) was employed in order to confirm the catalyst morphology. Also, Energy Dispersive Spectroscopy (EDS) to confirm the presence of Titanium and Oxygen in the synthesized catalyst as well as Brunaer Emmett Teller (BET); surface area measurements.

p-Aminobenzoic Acid (PABA) Degradation

A $5x10^{-5}$ M PABA solution was prepared and mixed with different quantities of TiO_2. The solution was stirred during 30 minutes to reach adsorption/desorption equilibrium. After that pH was adjusted to, or close to, 6 with NaOH 1M or HCl 1M. After that, H_2O_2 were added to provide the oxygen source. Once the reaction has started, it should take place in an isolated environment where the only light that its receives becomes exclusively from the light bulbs placed. Samples were collected every ten minutes to observe the degradation path. The catalyst loading studied range from 0.4 g/L to 1.2 g/L.

4. RESULTS:

Characterization of Titanium dioxide nanwires

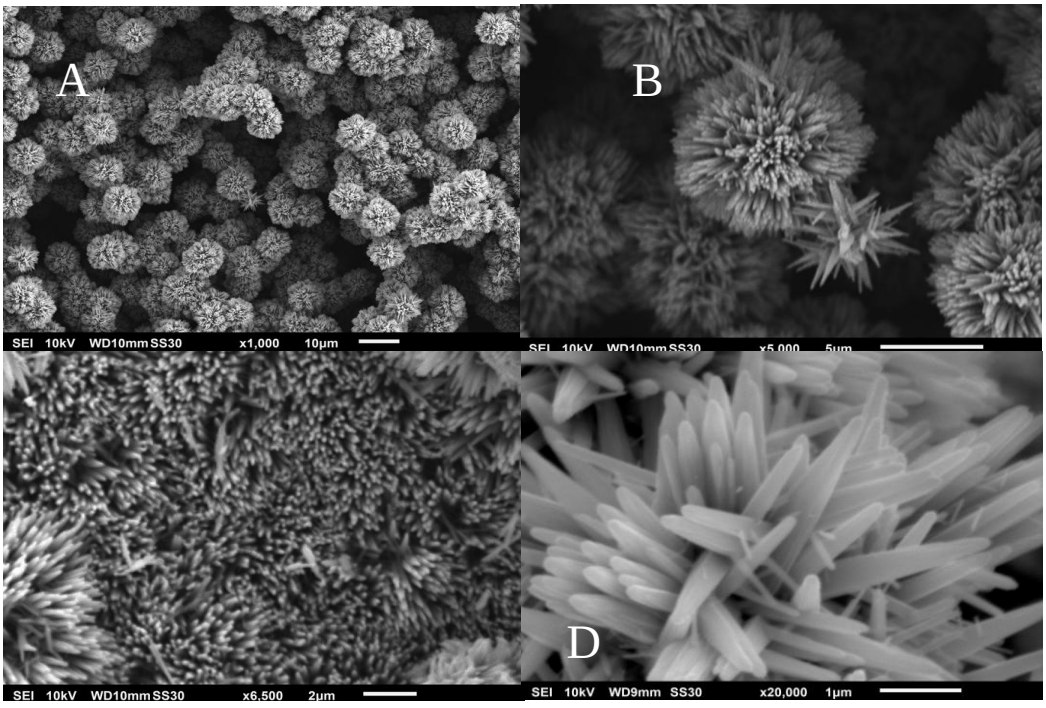

Figure 1: SEM images for TiO_2 nanowires at diferent magnifications.

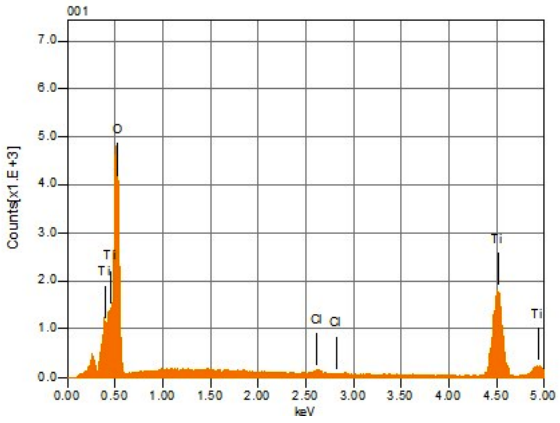

Figure 2: EDS analysis for TiO_2

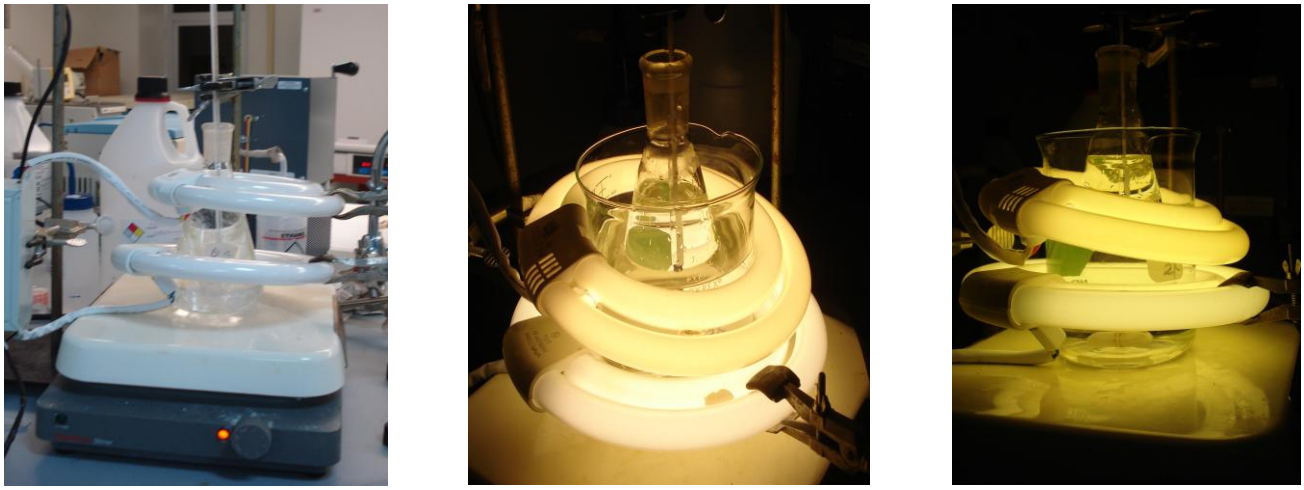

Figure 3. Photocatalysis Ensemble

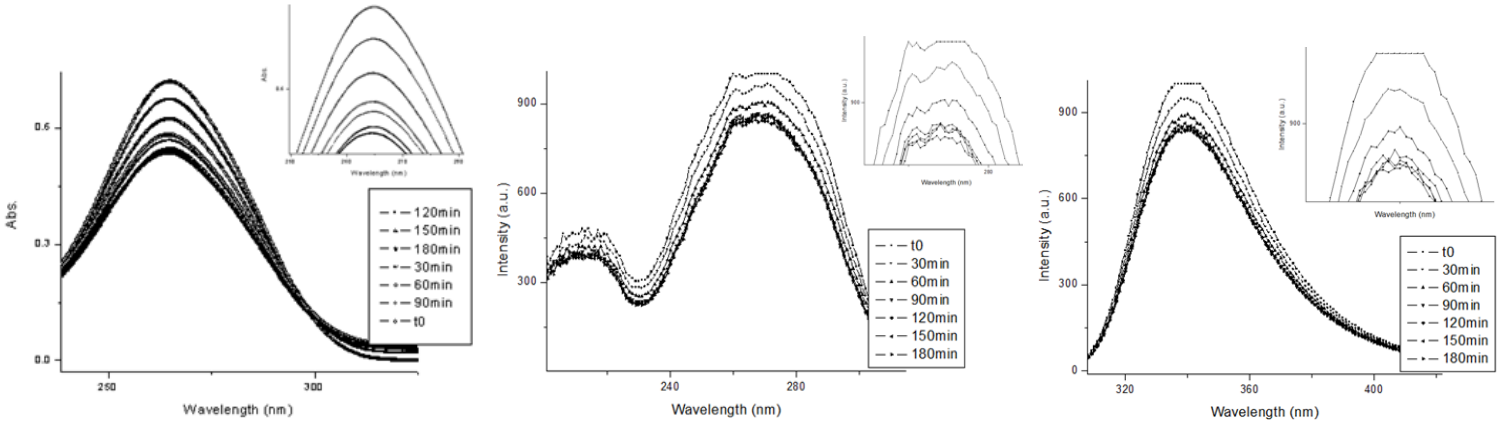

Figure 4: UV spectrum, excitation spectrum, and emission spectrum with 0.6 g/L of TiO_2 in PABA solution.

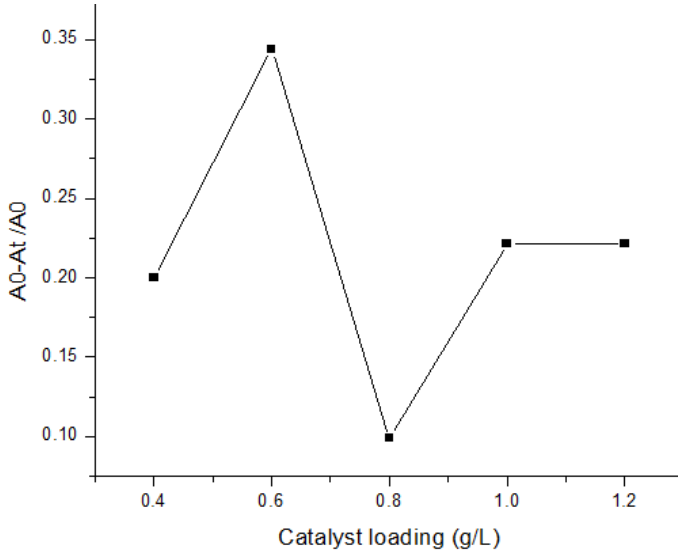

Figure 5: Graph showing the catalyst loading vs. the absorption raten in UV spectrum.

5. DISCUSSION

TiO_2 Nanowire Characterization

Titanium dioxide nanowires was successfully synthesized with a high surface area (584 m^2/g). Scanning Electron Microscope (SEM) was used to morphology of the catalyst obtained. Their qualitative characteristics consisted in two forms; spread on the substrate (Figure 1C) and spheric forms (Figure 1A). From the images, it can be observed that the growth of the TiO_2 nanowires start attaching to the silica substrate (Figure1C), and once covered, nanowires continued to grow over each other and later, attaching themselves into a spheric form (Figure 1B and 1D).

For the Energy Dspersive Spectroscopy analysis (Fig. 2) it can be observed that Titanium and Oxygen are present representin the Titanium dioxide. However, Chlorine is also present possibly due to its abundant presence in the reaction.

p-Aminobenzoic Photocatalyzed Degradation

Referring to Figure 4, in general, the degradation of p-Aminobenzoic Acid was successful, hence the concentration of the photo catalyzer in solution, because its efficiency increases proportionally with an increase in concentration, but minimizes it once passed the saturation limit for the Titanium dioxide to be able to function properly. Regarding figure 5, the chart represents the efficiency in degradation of PABA for the different catalyst loading studied. Because of the tendency of the nanowires as catalysts for photodegradation, its efficiency increases with more concentration, but after the optimum amount, which reports its best effectiveness, it decreases its features and does not allow the reaction to proceed properly. A few things, such as the ambient, temperature, pressure, and others, can influence in the reaction.

Regarding fluorescence spectroscopy, it has seem that water is the best effective medium for the catalysis process, because of the strong amount of electrons it possesses. The morphology of the nanowires provides a superficial area that is satisfactory for the degradation process. The “little spikes” found in the catalyst allows the molecules to attach to it and carry out the desired process (Linsebigler A.L. et. al. 1995). In our experimentation, we used a low concentration of peroxide but it was sufficient

to carry out degradation and for us to see a considerable change in the PABA concentration and for the Titanium dioxide to be a good catalyst. This being said, we can assume that our Titanium dioxide was a good catalyst, even though the parameter for the synthesis methodology can change its purity.

6. CONCLUSION

By incrementing the temperature to 180ºC and reduced the time in the oven to 2 hours, we obtained similar results than doing the same process but with a temperature of 150ºC in 4 hours (Cotto-Maldonado, M.C. 2012). Therefore, we managed to create the same catalyst material but in a more environmentally friendly way. With the photocatalysis procedure, we found that the optimum amount of catalyst used to degrade 1 liter of p-Aminobenzoic Acid was 0.6g of Titanium dioxide. This is supported by the calculations and the graph obtained from the spectrums done to show a comparison between the amounts used in the different reactions. We can say that the Titanium dioxide varies within the methodology because it has been proven that the efficiency of the photocatalysis depends on the method used during the synthesis. Our method was good, even with the low concentration of peroxide used; we can see a satisfactory degradation rate of our p-Aminobenzoic Acid solution, therefore we can say that or catalyst was good. The procedure is straightforward and very effective with 0.6g/L of Titanium dioxide in PABA solution. Photocatalysis and nanotechnology have become very important fields for water remediation and are to continue to be part of modern environmental research. In the future we would like to change the parameters to see if we can obtain a better synthesis and an even more efficient degradation rate.

7. FUTURE WORK

The photodegradation reactions of organic pollutants may take place through the formation of harmful intermediates that are more toxic than the original compounds. Therefore the knowledge on the identities of the intermediates is a must in photocatalytic degradation (GC-MS).

REFERENCES

A.K. Gupta, A. Pal, C. Jin, Y. Sahoo, 2006. Dyes Pigm. 69: 224-232.

Anastas P.T and Warner , J.C. 1998. Green Chemistry: Theory and Practice , Oxford University Press, 30.

Arabian Journal of Chemistry. 2012. King Saud Univerity.

Balmer M, Buser HR, Müller MD, Poiger TH. 2005. Occurrence of some organic UV filters in waste water, in surface waters, and in fish from Swiss lakes. Environ Sci Tchnol (39): 953-962.

Buser HR, Balmer M, Schmid P, Kohler M. 2006. Ocurrence of UV filters 4-methylbenzylidene camphor and octocrylene in fish from various Swiss rivers with inputs from wastewater treatment plants. Environ Sci Technol. 40: 1427-1431.

Chao Min, T. Abdul Rahman, M. 2011. Roles of Titanium dioxide and ion-doped titanium dioxide on photoatalytuc degration of organic pollutants (phenolic compounds and dyes) in aqueous solutions: A review. Journal of Alloys and Compounds. (509) 1648-1660.

Cotto-Maldonado, M.C. 2012. Heterogeneous catalysis applied to advanced oxidation processes (AOPs) for degradation of organic pollutants. Universidad del Turabo, 52

D.A. Lambropoulou, D.L. Giokas, V.A. Sakkas, T.A. Albanis, M.I. Karayannis. 2002. Gas chromatographic determination of 2-hydroxy-4-methoxybenzophenone and octyldimethyl-p-aminobenzoic acid sunscreen agents in swimming pool and bathing waters by solid-phase microextraction, J. Chromotogr. (967) 243-253.

Daughton, CG. 2004 Non regulated water contaminants: emerging research Environmental impact assessment review 24, 711-732.

Deng, Y., 2009. Advance oxidation processes (AOPs) for reduction of organic pollutants in landfill leachate: A review, International Journal of Environment and Waste management (4), 366-384.

Diaz-Cruz MS, Llorca M, Barcelo D. Organic UV filters and their photodegradates, metabolites and disinfection by- products in the aquatic environment. Trends Anal Chem (208) 27:873-87.

Díaz-Cruz MS, Llorca M. 2009. Chemical analysis and Eco toxicological effects of organic UV absorbing compounds in aquatic ecosystems. Trends Anal Chem (28): 708-717.

E. Rossetto, D.I. Petkowitz, J.H.Z dos Santos, S.B.C Pergher, F.G. Penha. 2006 Appl. Clay Sci. 48: 602-606.

Fujishima A., Rao T.N., Try D.A. 2000. Titanium Dioxide Photocatalysis. Journal of Photochemistry and Photobiology C Photochemistry Reviews (1): 1-21.

G. Centi and S. Perathoner. 2003. "Catalysis and Sustainable (Green) Chemistry", Catalysis Today, Vol. 77 (4): 287-297.

G.J. Hutchings. 2007. "A Golden Future for Green Chemistry " Catalysis Today, Vol. 122, (3-4):196-200. Doi:10.1016/j.cattod.2007.01.018

Goi, A. Trapido, M. Tuhkaken, T. 2004. Adv. Environ. Res. 8: 303-311.

Guillard C., Lachheb H., Houas A., Elaloui E., Hermann J-M. 2003. Influence of Chemical Structure of Dyes, pH and of Inorganic Salts on their Photocatalytic Degradation by TiO_2 Comparison of the efficiency of Powder and Supported TiO_2. Journal of Photochemistry and Photobiology: (158): 27-36.

H. Chun, W. Yizhong, T Hongxiao. 2009. Chemosphere (41):1205-1209.

H. Lachleb, E. Puzenat, A. Houas, M. Ksibi, E. Elaloui, C. Guillard, J.-M. Herrmann. 2002. Appl. Catal., B39 75-90.

Hoffman, M,R., Martin, S.T., Choi, W., Bahnemann, D,W. 1995. Environmental applications of semiconductor photocatalysis Chem. (95): 69-96.

J. Auvinen, L. Wirtanen. 2008. Atmos. Environ. (42): 4101-4112.

Kharissova, O.V., Rasika Dias H.V., Kharisov B.I., Olvera Pérez B., Jiménez Pérez V.M. 2013. The greener synthesis of nanoparticles. Trends in Biotechnology. 31 (4): 240-248.

Levine, A,D., Asano,T. 2004. Recovering sustainable water from wastewater. Environmental Science and Technology (38): 201A-208A.

Linsebigler A.L. et. al. 1995. Photocatalysis on TiO_2 surfaces: principal, mechanism, and selected results. The Chemical Review (95): 735-758

M. Karkmaz, E. Puzenat, C. Guillard, J.M Herrmann. 2004. Appl. Catal. (B51): 183-194.

M.E. Carlotti, E. Ugazio, l. Gastaldi, S. Sapino, D. Vione, I. Fenoglio, B. Fubini, J. photochem. 2009. Photobiol. (B96):130-135.

Osgood PJ, Moss SH, Davies DJG. 1982. The sensitization of near-ultraviolet radiation killing of Mammalian cells by the sunscreen agent para-aminobenzoic acid. J Invest Dermatol (79): 354-357.

P.T.Anastas, L.B. Barlett, M.M. Kirchoff and T.C. Willliamson. 2000. "The role in catalysis and design development, and implementation of Green Chemistry", Catalysis Today, Vol. 55 (1-2): 11-22.

Plagellat C, Kupper T, Furrer R, de Alencastroa LF, Grandjean D, Tarradellas J. 2006. Concentrations and specific loads of UV filters in sewage sludge originating from a monitoring network in Switzerland. Chemosphere; (62): 915-925.

Poiger T, Bser HR, Balmer ME, Bergqvist PA, Müller MD. 2004. Occurrence of UV filter compounds from sunscreens in surface waters: regional mass balance in two Swiss lakes. Chemosphere; (55): 951-963.

R.M. Mohamed, I.A. Mkhalid, J. 2010. Alloys Compd. (501): 143-147.

S. Ray, J.A. Lalman, N. Biswas. 2009. Chem. Eng. J. (150): 15-24.

Y. Liao, W. Que, J. 2010. Alloys Compd. (505) 243-248.

Zhang S, Chen J, Qiao X, Ge L, Cai X, Na G. 2010. Quantum chemical investigation and experimental verification on the aquatic photochemistry of the sunscreen 2-phenylbenzimidazole-5-sulfonic acid, Environ SciTechnol. (44) :7484-90.

Authorization and Disclaimer

Authors authorize PREC to publish the paper in the internship proceedings. Neither PREC nor the editors are responsible either for the content or for the implications of what is expressed in the paper.

Production of Biodiesel from Vegetable Oils and its Efficiencies

Steven De Jesús Santiago
Universidad del Turabo, Gurabo, PR, stevenpr_1@hotmail.com

Dayna M. Ortiz Rodríguez
Universidad del Turabo, Gurabo, PR, Mentor

Dr. Francisco M. Márquez-Linares
Universidad del Turabo, Gurabo, PR, Mentor

ABSTRACT

One of the main objectives of the scientific community is to find alternatives energy sources to lose or reduce the use of fossil fuels. The production of biodiesel is a viable, economic and environmental friendly way to reduce the harmful emissions to the atmosphere. Biodiesel was produce with three unused vegetables oils (olive, sunflower and corn) with a transesterification process using NaOH as a catalyzer and 5:1 oil to methanol ratio. To ensure the quality of the product, four tests were conducted: methanol, water, pH and viscosity. Efficiency and gas emissions test were done with a Gunt Hamburg CT110 diesel motor. Best efficiency was archived by sunflower biodiesel, followed by corn and finishing with olive. CO_2 emissions that could affect the environment were less than 4.10% for the three vegetable oils.

Keywords: Biodiesel, transesterification, vegetable oils, quality test, efficiency.

1. INTRODUCTION

One of the main debates in the world is how we can lose the dependency of fossil fuels because: CO_2 emissions, it is limited resource, price is constantly increasing, it is not available in all countries, and emissions can have carcinogenic effects. Because of these problems the study and research of alternative fuels like biodiesel is important. Biodiesel (fatty acid methyl esters) is a fuel that can be made by transesterification of triglycerides from vegetable oils, animal oil, waste vegetables oil (WVO) and animal fats (J. A. Colucci, et al., 2005). Biodiesel can be used in almost any diesel powered vehicle without or with little rearrangements of the motor (Calvo, 2000). The beneficial properties of this renewable fuel are many: it does not produce practically any CO_2 emission, sulfur or hydrocarbons emissions, is biodegradable thus spillages will not be a big problem, the storage and transportation is easier too (J. M. Encinar, et al., 2002). One of the main objections of the society for the use of biodiesel is the fuel versus food debate. The main drawback against biodiesel is the increasing price of the food market because the threat of the fuel market, but is being overshadowed by the creation of biodiesel from waste oil and the usage of nonedible crops.

The process from which glycerol and esters decompose from the large molecules of triglycerides to make glycerin and biodiesel is called transesterification (figure 1). The two main alcohols that are used in this process are methanol and ethanol. Ethanol can be used as a biosubstitution to methanol but it is more difficult to find and costlier than methanol. Most used catalyzers are in two groups: bases and acids; one substitution to sodium hydroxide is potassium hydroxide, the acid that have been more investigated is sulfuric acid but it needs to be used at a high concentration and its handling needs to be cautious.

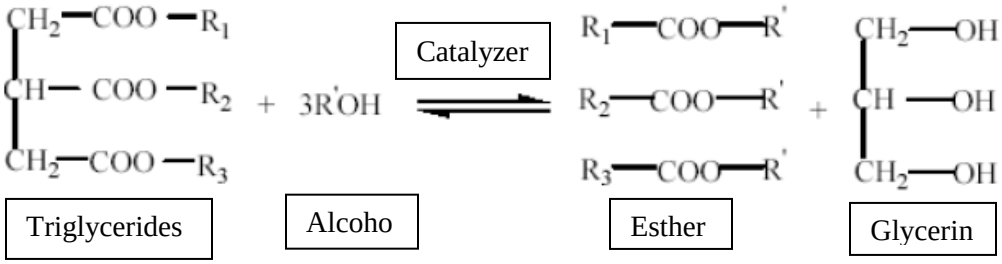

Figure 1: Transesterication Processes

Problems with biodiesel may occur if used at low temperatures because of the solidification of the fuel (A. T. Madsen, 2011). This happens because most vegetable oils are high in saturated fats and these fats are solid at room temperature. Some of the vegetable oils used in the production of biodiesel are jatropha, sunflower, rapeseed, sugarcane, palm, switchgrass, canola, corn, cottonseed and soybean (P. D. Patil, et al., 2009) Canola and rapeseeds are the oils that have less saturated fats and as a biodiesel have greater performance in low temperature environments (Li. E, 2009). Many anti-freeze or anti gel additives are available to increase the performance of biodiesel at low temperatures like: Flozol 503, BioFlow 875, MCC P205 and Arctic Express (D. S. Shrestha, et al., 2008).

2. EXPERIMENTAL SETUP

2.1 Materials. Three unopened vegetables oils were used: 100% extra virgin olive oil, pure sunflower oil and 100% natural corn oil. NaOH (sodium hydroxide) was used in pellets (ACS certified from Fisher Scientific 99.3%). CH_4O anhydrous (methanol) (ACS certified from Fisher Scientific 99.9%). Viscosity measurements were done with Cannon-Fenske viscosimeters. The pH measurements were made by an electrode pH meter (Mettler Toledo). Measurements of the efficiency and gas emissions were made by a Gunt Hamburg CT110 diesel motor.

2.2 Procedure. 5:1 oil to methanol ratio was made and mixed with 1.75g of NaOH. 500 mL of each oil was measured and heated in until it reached 70°C, this was done because many commercial oils come with water to maintain pureness of the oil. When the beaker with oil reached 70°C it was left to rest until it reached 40 °C. Sodium methoxide (CH_3ONa) was made by mixing 100 ml CH_3OH (methanol) and 1.75 g NaOH (see table 1 for the exact quantities).

Table 1

Vegetable Oils	NaOH (± 0.0001 g)
Olive	1.7541
Corn	1.7504
Sunflower	1.7514

It was verified that the CH_3ONa did not have any particles of NaOH. Each CH_3ONa was mixed with the oils and stirred and heated for two hours; its temperature remained between 35°C and 40°C. The result was a homogenous solution and then it was put into a separation funnel for two days. Two different phases were in the separation funnel: in the bottom $C_3H_8O_3$ (glycerine) on top of it there is biodiesel (methyl esters).

2.2.1 Quality Tests All the quality tests were accomplished using The Biodiesel Handbook. The first test is the methanol quality test which consists in mixing 9:1 methanol to biodiesel ratio and stir for a few seconds. If

residues of oil are in the bottom it means that not all the oil reacted with the CH_3ONa and the biodiesel needs to be reprocessed. The second quality test that was conducted is the water quality test which consists in mixing 1:1 water to biodiesel ratio, stir for a few seconds it is supposed to have two separated layers or two layers with a thin as a paper interface between. If they do not pass the test it could be due to incomplete reactions, the use of too much catalyst or both (K. Addison, 2013). None of our biodiesel passed any of the quality tests, a reprocess was needed because not all the oil reacted with the CH_3ONa. If they passed you can go directly to washing and drying steps.

2.2.2 Reprocess: Reprocess takes place when methanol or water quality test did not pass. It is done because not all the oil reacted with methanol and the pH, or suspended particles, in the biodiesel could damage the motor. If oil is in the biodiesel this could increase the viscosity and lower the flash point which is detrimental for the motor (D. Darnoko and M. Cheryan, 2000). The reprocessing is made by adding 60% of the methanol added the first time (60ml). After separating glycerin from biodiesel and adding 60ml of methanol to the biodiesel, it was stirred with a magnetic whisk and heated up to 35°C to 40°C. The solution was put in a separation funnel for one day. In the separation funnel was glycerin and biodiesel, it was observed that there is less glycerin because this was the second time that methanol is added and this solution has less triglycerides than the first solution. After glycerin is separated from biodiesel the same quality test were conducted and all the biodiesels passed them. Temperatures of the room, where the separation was made, must be above 25°C. This is very important because our room temperature was at 20°C and solidification/gelling of the glycerin was seen, also the glycerin did not maintained in the bottom of the separation funnel and it was needed to filter the biodiesel with a filter paper.

2.2.3 Viscosity, washing, pH and drying biodiesel. After biodiesel passed the first two quality test, the next step is to wash it. First, the viscosity of the biodiesel was tested with a Cannon-Fenske—viscosimeter.Washing is made because the presence of unconverted triglycerides, diglycerides, monoglycerides, glycerol, water, and many other undesired substances remains in the catalyst. Sterol glucosides and natural antioxidants, could cause significant engine damage by the consequent loss of power (H. Shi, et. al, 2012). Before washing, it is important to measure the pH because washing the biodiesel will decrease its pH, and the pH is needed to be in 7.0 (neutral) since it could damage the engine valves. Washing was made by doing one preliminary washing test for each biodiesel, with 50 ml biodiesel and 1/3 of 50ml water (16.67ml of water). After stirring this solution for 5 minutes it was put in a separation funnel for 1 hour. In the separation funnel now is appreciated water in the bottom and biodiesel on top. Water is separated from the biodiesel and pH measurements of the biodiesel were conducted having all in the range set, which was 6.80-7.20 of pH. The next step was to dry the biodiesel. Drying is important because water in the motor and all other residues explained above could damage the motor. The procedure consisted in to put the biodiesel at 48°C to evaporate all the remaining water in the biodiesel. If the biodiesel is not cloudy, is a good sign that the residues of water had been evaporated.

2.2.4 Test in motor. Biodiesel was test in a Gunt Hamburg CT110 diesel motor. In this motor many things can be tested like: efficiency, volumetric efficiency, fuel-air ratio, gas emissions and temperature of the fuel. 300 mL of the biodiesel were used to carry the tests.

3. RESULTS AND DISCUSSIONS

It is important to mention that the reactions were tested with different amounts of NaOH. 0.25g, 0.50g, 1.00g and 1.75g of NaOH were tested but 1.75g was seemed to be the best amount for the reaction, because it produces less soap in the washing and in the water test. Solidification and gelling of the glycerin was demonstrated by heating and cooling glycerin and seeing that it solidifies at about 20°C and remains liquid above 25°C. Because of this the biodiesel contained little strings of glycerin, they were floating and separating them in a separation funnel was impossible. It was needed filtration with a filter paper to maintain pureness of the oil. Quality tests passed after reprocessing the biodiesel, as they can be appreciated in figure 2.

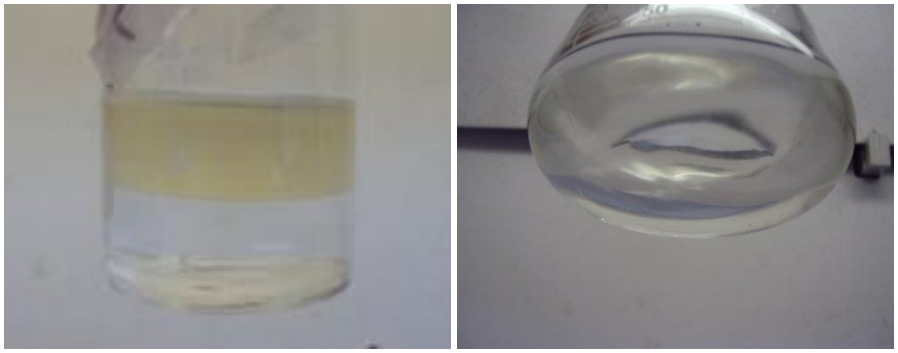

Figure 2: Methanol and water quality tests

Dynamic viscosity test were done on all oils at two temperatures: 20°C and 40°C. Results can be seen in table 2 and table 3. Viscosity measurements were done with Cannon-Fenske viscosimeters.

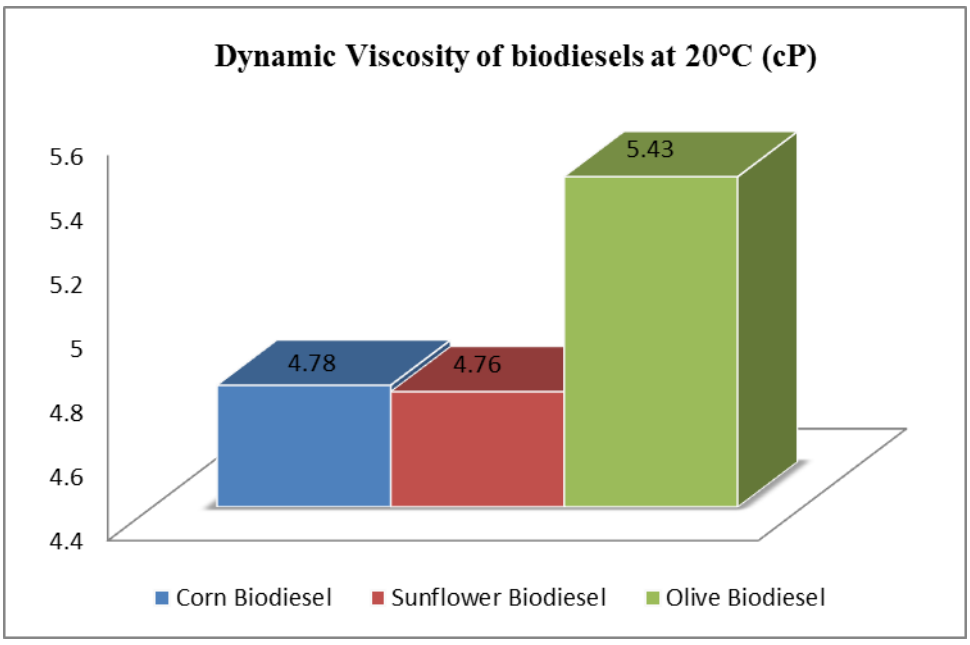

Figure 3

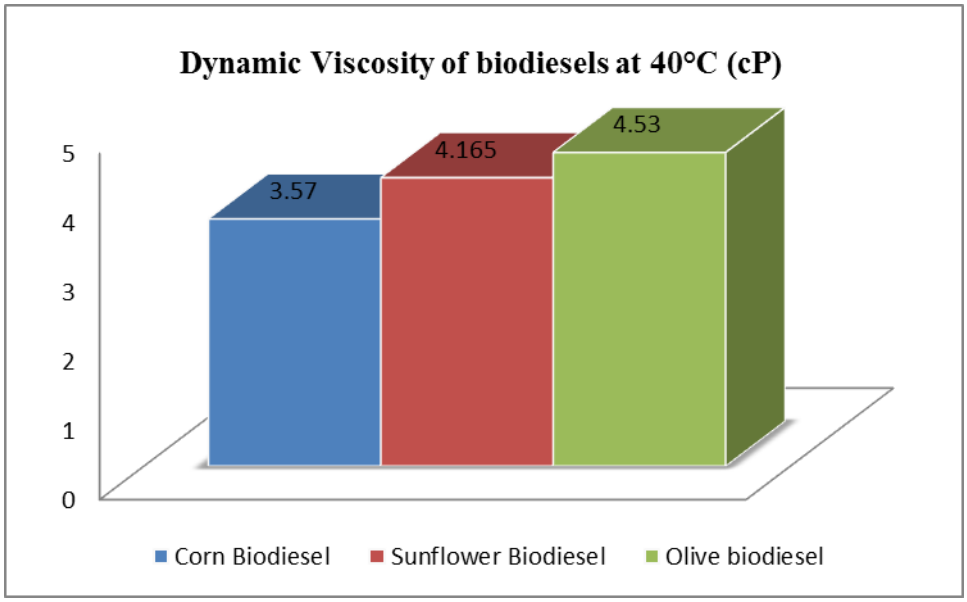

Figure 4

The viscosity of a fluid is a measure of its resistance to displace (A. P. Ferreira et al., 2009). In figures 3 and 4 it is seen that at higher temperatures the viscosity drops. It is appreciated that olive biodiesel has the higher viscosity in the two temperatures. Sunflower biodiesel has the lower viscosity at 20°C and Corn biodiesel has the lower viscosity at 40°C. Sunflower and corn biodiesel are expected to have the best results because of its lower viscosities.

Efficiency and gas emissions tests at the motor were conducted; results are in figure 5 and table 2 respectively.

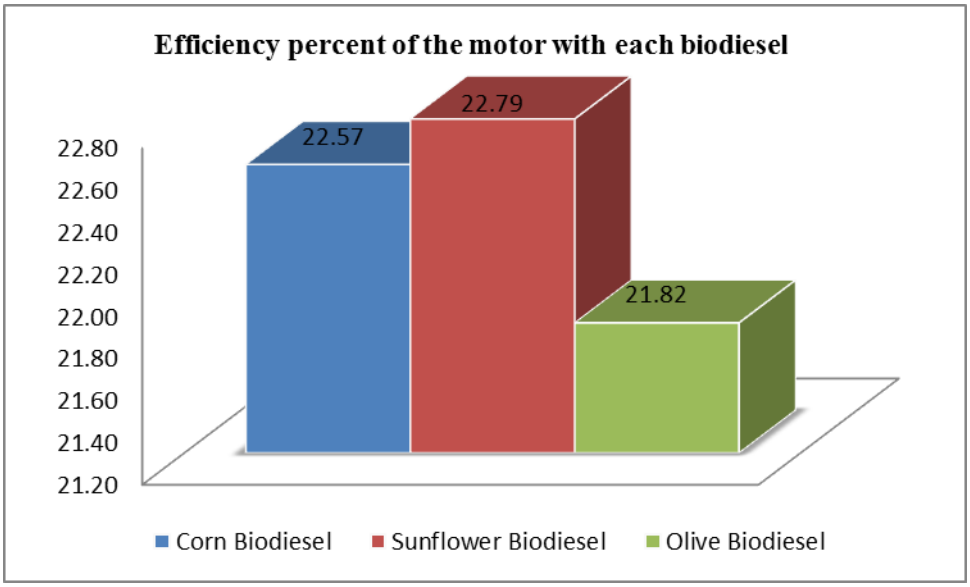

Figure 5

Table 2

Average gas emissions of each fuel			
	Corn	**Sunflower**	**Olive**
% Vol CO	0.053	0.053	0.14
%Vol CO_2	3.99	3.45	4.09
%Vol 0_2	15.69	15.56	15.49

Figure 5 shows that the best efficiency was archived by sunflower biodiesel. The lowest efficient was olive biodiesel. It can be seen in table 2 that Olive got the greater CO and CO_2 emission.

4. CONCLUSION

All the biodiesel passed all three quality tests, established by The Handbook of Biodiesel. Best efficiency was archived by sunflower biodiesel, followed by corn and finishing with olive. Viscosity tests disclosed that at 20°C sunflower was the lowest viscosity which is better for the motor engine. At 40°C, corn archived the lowest viscosity. Olive low viscosity affected the efficiency of the motor because olive biodiesel always showed the highest viscosity on both tests and efficiency. Gas emissions test demonstrated that biodiesel did not emit the sufficient volume of gases that could affect the environment. All biodiesel behave almost the same in average gas emissions.

Future tests will be conducted with different amounts of methanol and catalyzer and the temperature will be controlled all the time.

REFERENCES

A. P. Ferreira, C. R. da Costa Rodrigues, D. M. do Espírito Santo, J. R. Real Siqueira, R.Guimares Pereira, L. H. Paraguassu de Oliveira. (2009). metrological approach in the characterization of viscosity of corn biodiesel relative to temperature, using capillary viscometers. *Fundamental and Applied Metrology*. Vol. 34 pp. 102-106.

Calvo, MS. (2000). "Tratado de Reciclado y Recuperación de Productos de los Residuos". *Mundi-Prensa Libros*. Pp. 211.

D. Darnoko and M. Cheryan. (2000). "Kinetics of Palm Oil Transesterification in a Batch Reactor". *JAOCS*. Vol. 77.

D. S. Shrestha, J. Van Gerpen and J. Thompson. (2008). "Effectiveness of Cold Flow Additives on Various Biodiesels, Diesel, and Their Blends". *American Society of Agricultural and Biological Engineer*. Vol. 51(4), pp. 1365-1370.

H. Shi, M. Yuan and T. Wang. (2012). "Design of biodiesel production processes by base-catalyzed transesterification". *Advanced Materials Research*. Vols. 512-515 pp. 510-514.

J. A. Colucci, E. E. Borrero, and F. Alape. (2005). "Biodiesel from an Alkaline Transesterification Reaction of Soybean Oil Using Ultrasonic Mixing". *JAOCS*. Vol. 82, no. 7, pp. 525-530.

J. M. Encinar, J. F. González, J. J. Rodríguez, and A. Tejedor. (2002). "Biodiesel Fuels from Vegetable Oils: Transesterification of Cynara cardunculus L. Oils with Ethanol". *American Chemical Society*. Vol. 16, pp. 443-450.

K. Addison. http://journeytoforever.org/biodiesel_vehicle.html#reprocess. 15/june/2013.

Li E., Xu ZP, Rudolph V. (2009). "MgCoAl-LDH derived heterogeneous catalysts for the ethanol transesterification of canola oil to biodiesel". *Appl. Catal*. 42–49(2009).

P. D. Patil, V. G. Gude, and S. Deng. (2009)."Biodiesel Production from Jatropha Curcas, Waste Cooking, and Camelina Sativa Oils". *American Chemistry Society*. Vol. 48, pp. 10850–10856.

Authorization and Disclaimer

Authors authorize PREC to publish the paper in the internship proceedings. Neither PREC nor the editors are responsible either for the content or for the implications of what is expressed in the paper.

August 19, 2013

SUMMER INTERNSHIP

Clean Technologies Research

2013

Mentors

Amaury Malavé Sanabria, PhD
Executive Director of Puerto Rico Energy Center
Universidad del Turabo
Phone (787)743-7979 Ext. 4731

Carlos J. Olivo Delgado, PhD
Associate Dean
School of Science and Technology
Universidad del Turabo
Phone: (787) 743-7979 Ext. 4167

Edwar Romero, PhD
Associate Professor and
Mechanical Engineering Master's Director
Mechanical Engineering Department,
Universidad del Turabo
Phone: (787) 743-7979 Ext. 4733

José R. Pérez Jiménez, PhD
Director Interdisciplinary Research Institute
Director Puerto Rico Institute for
Microbial Ecology Research
Associate Professor,
School of Science and Technology
Universidad del Turabo
Phone (787)743-7979 Ext. 4567

Ricardo Esbri Amador, Eng PE PA
Mechanical Engineer
esbri@hotmail.com

Abraham García
Candidate PhD Science and Technology

Dayna M. Ortíz Rodríguez
Candidate MS Environmental Science

Loraine Soto Vázquez
Candidate MS Environmental Science

Ián Gutiérrez Molina
Technical Director

Students

Alan López García
Computer Engineering
Universidad de Puerto Rico
Mayagüez Campus

Bryan Santana Rivera
Mechanical Engineering
Universidad del Turabo

Dennis J. García Torres
Chemistry
Universidad del Turabo

Edaris Rodríguez Izquierdo
Associate Degree in Biotechnology
Universidad del Turabo

Euvelisse Jusino Del Valle
Chemistry
Universidad de Puerto Rico
Rio Piedras Campus

Gelson Díaz Lozada
Mechanical Engineering
Universidad del Turabo

Jemyelbi L. Figueroa
Chemistry
Universidad del Turabo

Nicole M. Delgado Rodríguez
Biology
Universidad del Turabo

Sigfredo Nieves Taboas
Mechanical Engineering
Universidad del Turabo

Steven De Jesús Santiago
Mechanical Engineering
Universidad del Turabo

PREC

August 19, 2013

SUMMER INTERNSHIP

Clean Technologies Research

2013

Students

Tanairí Cabrera Guadalupe
Associated Degree in Computers
Technology and Networks
Universidad del Turabo

Tracey Rodríguez Franqui
Chemistry
Universidad del Turabo

Víctor E. Zayas Rodríguez
Electrical Engineering
Universidad del Turabo

Scientific reviewers

Alizabeth Sánchez PhD
School of Business and Entrepreneurship
Universidad del Turabo

Amaury Malavé Sanabria, PhD
Executive Director of Puerto Rico Energy Center
Universidad del Turabo

Gary W. Gervais, PhD
Universidad de Puerto Rico
Rio Piedras Campus

Marcelo Suarez, PhD
Universidad de Puerto Rico
Mayagüez Campus

Mark Lau, PhD
School of Engineering
Universidad del Turabo

Yarilyn Cedeño, PhD
Universidad Interamericana

Yazan Hihazi, PhD
School of Engineering
Universidad del Turabo

PREC

August 19, 2013

SUMMER INTERNSHIP

Clean Technologies Research

2013

Collaborators

Antonio Seda

Armando Soto

Carlos J. Olivo Delgado

Darlene Muñoz Villafañe

Ián Gutiérrez Molina

Josefina Melgar

Miguel Cotto Morales

Miguel Delgado

Sandra Méndez

Sandra R. Pedraza Torres

Suheilie Rodríguez González

Yomarie Bernier Casillas

PREC

PUERTO RICO ENERGY CENTER

2013 Summer Internship

Universidad del TURABO

INTECO

PROGRAM
MASSIE CHAIR OF EXCELLENCE
GRANT DE-NA0000672

PUERTO RICO ENERGY CENTER

2013 Summer Internship

Universidad del TURABO

INTECO

PROGRAM
MASSIE CHAIR OF EXCELLENCE
GRANT DE-NA0000672